HHS Public Access

Author manuscript

Nanoscale. Author manuscript; available in PMC 2018 October 19.

Published in final edited form as:

Nanoscale. 2017 October 19; 9(40): 15226–15251. doi:10.1039/c7nr05429g.

Redox-active Nanomaterials for Nanomedicine Applications

Christopher M. Sims[1,*], **Shannon K. Hanna**[1,#], **Daniel A. Heller**[2,3], **Christopher P. Horoszko**[2,4], **Monique E. Johnson**[1], **Antonio R. Montoro Bustos**[1], **Vytas Reipa**[1], **Kathryn R. Riley**[5], and **Bryant C. Nelson**[1,*]

[1]Material Measurement Laboratory, National Institute of Standards and Technology (NIST), 100 Bureau Drive, Gaithersburg, MD 20899, United States

[2]Memorial Sloan Kettering Cancer Center (MSKCC), 1275 York Avenue, New York, NY 10065, United States

[3]Weill Cornell Medicine, Cornell University, 1300 York Avenue, New York, NY 10065, United States

[4]Weill Graduate School of Medical Sciences, Cornell University, 1300 York Avenue, New York, NY 10065, United States

[5]Department of Chemistry and Biochemistry, Swarthmore College, 500 College Avenue, Swarthmore, PA 19081, United States

Abstract

Nanomedicine utilizes the remarkable properties of nanomaterials for the diagnosis, treatment, and prevention of disease. Many of these nanomaterials have been shown to have robust antioxidative properties, potentially functioning as strong scavengers of reactive oxygen species. Conversely, several nanomaterials have also been shown to promote the generation of reactive oxygen species, which may precipitate the onset of oxidative stress, a state that is thought to contribute to the development of a variety of adverse conditions. As such, the impacts of NMs on biological entities are often associated with and influenced by their specific redox properties.

In this review, we overview several classes of nanomaterials that have been or projected to be used across a wide range of biomedical applications, with discussion focusing on their unique redox properties. Amongst the nanomaterials examined include iron, cerium, and titanium metal oxide nanoparticles, gold, silver, and selenium nanoparticles, and various nanoscale carbon allotropes such as graphene, carbon nanotubes, fullerenes, and their derivatives/variations. Principal topics of

[*]Authors to whom correspondence should be addressed: christopher.sims@nist.gov, 301-975-2671 (p). bryant.nelson@nist.gov, 301-975-2517 (p).

[#]Present address: Center for Tobacco Products (CTP), Food and Drug Administration (FDA) 10903 New Hampshire Avenue, Silver Spring, MD 20993, United States

discussion include the chemical mechanisms by which the nanomaterials directly interact with biological entities and the biological cascades that are thus indirectly impacted. Selected case studies highlighting the redox properties of nanomaterials and how they affect biological responses are used to exemplify the biologically-relevant redox mechanisms for each of the described nanomaterials.

Keywords

nanomedicine; redox mechanisms; biological response; reactive oxygen species; nanomaterials

Introduction

Nanomedicine, the medical application of nanotechnology, harnesses the properties of nanomaterials (NMs) for biomedical applications, including diagnostic assays, therapeutic delivery systems, and tissue engineering.[1–4] While NMs are renowned and utilized due to their remarkable properties, such as their optical, thermal, or magnetic properties, their redox properties are also pertinent to their safe and effective use in the biomedical sector.[5] One such biomedical application where NMs have been shown to have much promise is in antioxidant activity, specifically in the scavenging of reactive oxygen species (ROS).[6]

ROS are oxygenated redox active species that are produced in the body as normal byproducts of metabolic processes or accumulated from the environment.[7–9] Examples of ROS include hydrogen peroxide (H_2O_2), superoxide ($O_2^{\bullet -}$), singlet oxygen ($^1O_2$), and the highly reactive hydroxyl radical ($^{\bullet}OH$).[10] While ROS are widely used throughout the body as signaling molecules,[11] they can also damage biological entities (e.g. proteins, lipids, DNA).[7] Elevated levels of ROS and oxidative damage can result in oxidative stress, a state that is thought to contribute to the development of a variety of adverse human conditions, including cancer, neurodegenerative diseases, and cardiovascular diseases.[12–14] To counteract the often adverse effects of oxidative stress, several antioxidative mechanisms exist which serve to balance ROS levels.[15] Amongst these antioxidants are the superoxide dismutase (SOD), catalase (CAT), and glutathione peroxidase (GPx) families of enzymes.[9, 10, 15] Whereas SOD typically catalyzes the dismutation of $O_2^{\bullet -}$ into H_2O_2, CAT and GPx catalyze the decomposition of H_2O_2 into water.[9, 10] In the case of GPx, glutathione (GSH), a selenium-containing molecule, is oxidized to glutathione disulfide (GSSG). Antioxidant NMs have been shown to scavenge ROS via mechanisms analogous to that of the body's natural antioxidative mechanisms and are hence, sometimes described as having enzyme-mimetic activities.[16, 17]

The redox properties of NMs can also be pro-oxidative, leading to the generation of ROS. This excessive generation would presumably lead to the disruption of the aforementioned antioxidant mechanisms, inducing the progression of oxidative stress and the previously described adverse effects associated with it.[18, 19] However, these pro-oxidative redox properties can also be harnessed for useful applications. One such example is the treatment of cancer (one such disease associated with oxidative stress) either through the direct production of ROS or via photodynamic therapy (PDT). PDT utilizes a photosensitizing (PS)

agent that has been localized to a tumor and the activation of that agent via light.[20] Specifically, the localized PS is excited by laser light of a suitable wavelength to form a singlet excited state photosensitizer (PS*).[21] The PS* then undergoes an intersystem crossing to form a triplet excited state (PS**) which can then either 1) induce electron transfer to the surrounding environment and generate ROS (typically free radicals such as $^{\bullet}OH$ or $O_2^{\bullet-}$), denoted Type I or; 2) undergo an energy transfer process with ground state $^3O_2$ to produce singlet $^1O_2$, denoted Type II.[21] Regardless of the mechanism of generation, these NM-generated ROS could then proceed to damage and destroy vital tumor biomolecules, functioning as cytotoxic agents if applied specifically to cancerous cells.

In this review, we overview several classes of NMs that have been or projected to be used across a wide range of biomedical applications, with discussion focusing on their unique redox properties and their effects on biological systems. The NMs examined include iron, cerium, and titanium metal oxide nanoparticles (NPs), gold, silver, and selenium nanoparticles, and various nanoscale carbon allotropes such as graphene, carbon nanotubes (CNTs), fullerenes, and their derivatives/variations. These are amongst the most common NMs being researched for applications in nanomedicine. Principal topics of discussion include the chemical mechanisms by which these NMs directly interact with biological entities and the biological cascades that are thus indirectly impacted. Selected case studies highlighting the redox properties of nanomaterials and how they induce biological responses are used to exemplify the biologically-relevant redox mechanisms for each of the described nanomaterials. Each case study is described and discussed in detail, accompanied by commentary of the work's significance towards advancing our understanding of nano-bio redox mechanisms and their influence on nanomedicine modalities.

Iron Oxide Nanoparticles

Iron oxide NPs (IONs) are amongst the most heavily researched and potentially versatile NMs for biomedical applications, which range from magnetic resonance imaging (MRI) and cell tracking to targeted therapeutics and tissue engineering.[22, 23] Most of these applications exploit the IONs' interesting property of superparamagnetism, wherein the particles exhibit magnetism *only* in the presence of an external magnetic field, which ceases when this external field is removed.[24, 25] As such, it is possible to use superparamagnetic IONs (SPIONs) to generate heat when an alternating magnetic field is applied; alternatively, they may be directed to specific tissues/organs using an external magnetic field.[26, 27] Relative to other common paramagnetic elements/complexes (e.g., Cobalt, Nickel, Gadolinium-complexes), SPIONs are also thought to have reduced toxicity and increased biocompatibility;[28, 29] combined with their superparamagnetism and colloidal stability, they are quite appealing for applications in nanomedicine.[30, 31]

While most of these biomedical applications utilize the SPIONs' magnetic properties, their other physicochemical properties (e.g., size, surface chemistry, surface coating) have greater influence on their interactions with biological entities (e.g., proteins, cells, tissues).[31, 32] Highlighted amongst these properties is the redox chemistry of SPIONs, which heavily depends on the particles' chemical composition. SPIONs primarily exist in the forms magnetite (Fe_3O_4) or maghemite (γ-Fe_2O_3),[24, 25] both of which form inverse spinel

structures, where the oxygen anions are arranged as a face-centered cubic and the iron cations occupy interstitial tetrahedral and octahedral sites.[33] Given the structural similarities, the most apparent difference between the two forms are that magnetite contains both Fe^{2+} and Fe^{3+} ions, while the iron in maghemite is almost entirely in the Fe^{3+} state.[33] Systemic quantities of the two Fe oxidation states are important due to their role in catalyzing a series of ROS generating reactions, specifically the Fenton and Haber-Weiss reactions:[34, 35]

$$Fe^{2+} + H_2O_2 \rightarrow Fe^{3+} + OH^- + {}^{\bullet}OH \quad (1)$$

$$Fe^{3+} + H_2O_2 \rightarrow FeOOH^{2+} + H^+ \quad (2)$$

$$FeOOH^{2+} \rightarrow Fe^{2+} + {}^{\bullet}OOH \quad (3)$$

$${}^{\bullet}OOH \rightarrow H^+ + O_2{}^{\bullet-} \quad (4)$$

As shown, both Fe states can lead to ROS formation ($^{\bullet}OH$, $^{\bullet}OOH$, $O_2{}^{\bullet-}$), which can induce oxidative stress through various mechanisms described earlier. SPIONs have been shown to cause oxidative stress across many studies, including promotion of oxidative DNA damage in human lymphoblasts,[36] disruption of lysosomal and mitochondrial function in rat cardiomyocytes,[37] and apoptosis of human macrophage mediated by overactivation of the c-Jun N-terminal kinase (JNK) signaling cascade.[38]

While SPIONs have been shown to have toxic effects on biological systems, a key factor in the ability of SPIONs to cause oxidative damage is their ability to liberate free Fe. Coating the SPIONS with biocompatible compounds (e.g., lipids, polyethylene glycol (PEG), dextran) not only increases their colloidal stability and minimizes their nonspecific interactions with biomolecules,[25, 26] but also helps to reduce their degradation into free Fe, which produces more ROS relative to intact SPIONs.[39] While much research has been done to characterize the physicochemical properties of SPIONs with respect to the colloidal coating, their interactions with biological systems are difficult to ascertain since the nature of the interaction depends not just on the properties of the SPIONs, but also on the biological system itself.[28, 32, 38, 40–42] For example, PEGylated SPIONs have been found to increase DNA damage in mice lung tissue at a much lower degree as compared to non-PEGlyated SPIONs; in addition, negatively charged PEGlyated SPIONs were found to induce slightly more DNA damage than their positively charged counterparts.[40] However, another study of multiple human cell lines (HCM, BE-2-C, and 293T) found that the positively charged SPIONs led to lower cell viability relative to negatively charged SPIONs.[32] As such, the effects of SPION redox mechanisms will vary per the specific parameters of the overall system.

Previous studies had shown that SPIONs could catalyze oxidation of peroxidase substrates in acidic solutions in the presence of H_2O_2 through reaction (1); this SPION-based reaction was termed a peroxidase-like activity.[43] Likewise, under more neutral pH conditions, SPIONs lose their peroxidase-like activity and instead catalyze the disproportionation of H_2O_2 into H_2O and O_2; this reactivity was termed a catalase-like activity.[44] The catalase-like mechanism is proposed to occur through reactions (2) and (3) in combination with reaction (5) below:[45]

$$^{\bullet}OOH + {}^{\bullet}OH \rightarrow H_2O + O_2 \quad (5)$$

Based on these observations, Chen et al.[45] investigated the interaction of SPIONs with H_2O_2 in human glioblastoma cells, with the goal of devising a scheme to diminish the cytotoxic effects of the SPIONs. Using Fe_3O_4 and Fe_2O_3 SPIONs, the authors found that both types of particles were readily taken up by the cells after 12 h of exposure. Most of the SPIONs localized to the lysosomes. Viability assays showed that the Fe_2O_3 particles had little toxic effect on the cells, which were more than 85 % viable across all tested concentrations. Conversely, the Fe_3O_4 particles showed dose-dependent toxicity. These observations were supported by electron spin resonance (ESR) spectroscopy measurements conducted at pH 4.8 and pH 7.4 to mimic the environments of lysosome and cytosol respectively.[45] The ESR results showed that both types of SPIONs produced $^{\bullet}OH$ at pH 4.8, while the Fe_3O_4 particles produce more radicals (increased peroxidase-like activity) than their Fe_2O_3 counterparts (recall that Fe_3O_4 contains Fe^{2+} while Fe_2O_3 is fully comprised of Fe^{3+}). Interestingly, $^{\bullet}OH$ production was not observed at pH 7.4 for either type of SPION, which suggested a catalase-like activity. Under these conditions, it was believed that the SPIONs effectively functioned as a ROS scavenger (antioxidant activity) rather than a ROS producer (pro-oxidant activity). As such, along with the authors' findings that Fe_3O_4 particles are more toxic than Fe_2O_3 particles, the idea that SPIONs could be used to protect cells from oxidative stress under specific conditions was an important outcome of the study.

Building off of this, Huang et al.[46] sought to harness the toxic effects of SPIONs to improve the therapeutic effect of β-lapachone (β-lap), an anticancer drug which operates by inducing necrosis via poly(ADP-ribose) polymerase 1 (PARP1) hyperactivation. This mechanism operates through elevated levels of H_2O_2 and $O_2^{\bullet -}$. Fe_3O_4 SPIONs were synthesized and then incorporated into micelles comprised of poly(ethyleneglycol)-b-poly(2-(2-diisopropylamino) ethyl methacrylate (PEG-b-PDPA), a pH-sensitive amphiphilic copolymer. To test for pH-sensitive release of the SPIONs, Fe concentrations in buffers at pH 7.4, 6.2, and 5.0 were measured by atomic absorption spectrometry after 72 h. At pH 7.4, Fe ions were not observed, while Fe was found at the lower pH values in increasing quantities. The mechanism of release was attributed to the protonation of the PDPA segments of the polymer, leading to micelle dissociation and release of SPIONs, which could then be degraded to free Fe ions at the lower pH. The authors then treated lung carcinoma cells with the SPION-micelles, both with and without β-lap (which was also tested without SPIONs) for 48 h. After 4 h of incubation, >80 % of the SPION-micelles were localized in the endosomes (pH 5.5 to 6.3) and lysosomes (pH 5.0 to 5.5), although Fe

ion release was found to take longer (only 40 % of the total Fe ions were released at pH 5.0 after 48 h in the initial pH sensitivity test). A fluorescence assay indicated cells treated with SPION-micelles only showed no effect, while cells treated with β-lap only produced very little fluorescent signal; both findings suggest a limited production of ROS under their respective conditions. However, the cells treated with both β-lap and SPION-micelles had over 10-fold higher fluorescence intensity, suggesting a more than 10-fold increase in ROS levels. The massive increase in ROS production from the synergistic treatments was corroborated by long-term cell survival assays. Under experimental conditions, the cell survival rate fell from 72 % to 10 % when SPION-micelles were added to the β-lap treatment. When compared in combination with the previously discussed properties of SPIONs, these SPION-micelles show promise for use in theranostic nanomedicine against various cancer types.

However, heightened ROS levels as promoted by SPIONs are often detrimental to biological systems and impact their use in most of their designed applications. A recent study by Pongrac et al.[47] monitored several oxidative stress endpoints in mouse neural stem cells (NSCs) to investigate the impact of different surface functionalizations (uncoated, D-mannose-coated, and poly-L-lysine-coated) on SPION toxicity. Due to their ability to differentiate into many types of specialized cells, stem cells are the focus of much research attention for their use in regenerative medicine therapies.[48] Cell tracking via SPION-based MRI is one of the most promising methods for monitoring stem cell migration and differentiation, two essential processes in therapeutic stem cell treatment.[49] While viability assays did not show significant reductions in NSC viabilities across the SPION concentration levels examined, levels of glutathione (GSH) were greatly depleted. The authors also found significant decreases in superoxide dismutase (SOD) activity, with corresponding increases in glutathione peroxidase (GPx) activity; these observations indicated that the NSCs were under significant oxidative stress upon SPION treatment. Assessments of mitochondrial membrane potential (MMP) and cell membrane potential (CMP) changes, along with DNA damage measurements, substantiated the results of earlier experiments for the SPION-exposed NSCs, where severe detrimental effects of excessive ROS were seen for all SPIONs investigated. Interestingly, surface coating appeared to have little impact on the toxicity of the SPIONs, as significant differences between toxicity end points were not observed as a function of coating. Also of note were the authors' discussions regarding the possibility that underlying cellular functions could still be impaired despite "rough" toxicity end-points measurements (e.g., cellular viability, ROS levels) approaching their limit of detection.[47]

Umashankar et al.[50] also studied the effects of SPIONs on NSCs; specifically, the influence of Molday ION Rhodamine B (MIRB) (a commercially available SPION used for cell labelling, tracking, and MRI) on the survival and regenerative capacity of rat NSCs both *in vitro* and *in vivo*. While the NSCs could be detected when labeled at both doses (20 μg and 50 μg) of MIRB, the higher dose was found to increase MRI contrast signal, which seems to be an unsurprising result. The 50-μg dose significantly compromised the viability and proliferation of the NSCs *in vitro*, yet the 20-μg dose did not appear to affect these two cytotoxicity endpoints when compared to the untreated control NSCs. The ability of the MIRB-labeled NSCs to generate a differentiated cell type and morphology was assessed.

The 50-μg dosed NSCs featured substantial reductions in differentiated cells with the differentiated cells also having altered morphological characteristics. Curiously, despite no significant impact on the generation of differentiated cells, the 20-μg dosed NSCs exhibited differences in morphology compared to the control. In practice, these morphology alterations could have massive ramifications for *in vitro* production and *in vivo* grafting of SPION-labeled NSCs.[50] *In vivo* measurements of contrast signal, NSC graft size (a measure of NSC viability), and proliferation all generally agreed with the *in vitro* results: the 50-μg dosed group had more adverse outcomes than the 20-μg dosed group. In all circumstances, increased ROS production resulting from the presence of SPION was suggested to be the major contributor to the observed differences between the control and MIRB-treated NSCs.

While SPIONs are promising for several applications in the field of nanomedicine, these studies highlight their propensity to produce toxic amounts of ROS. While this toxicity can be utilized for cancer treatments, other applications will require greater control of toxicity mechanisms to enable translation of SPIONs into the clinical setting. As described earlier, controlling the chemical nature of the SPION coating (e.g., identity, charge) is just one approach to mitigate their toxicity. Other strategies under investigation include encapsulating SPIONs within liposomes, SPION surface passivation with shielding silica shells, and pretreatments to enhance antioxidant levels prior to SPION introduction.[51]

Cerium Oxide Nanoparticles

Cerium oxide NPs (CNPs) are widely used in industry as chemical mechanical polishing agents, in anticorrosion coatings, and as an additive in diesel fuel.[52] However, the potential benefits of CNPs for medical applications have only recently gained interest due to several studies that showed antioxidant properties in cell models.[53–55] These antioxidant properties result from the coexistence of Ce^{3+} and Ce^{4+} states on the surface of the particles,[56–58] which contribute to the high chemical reactivity of CNPs. While Ce^{4+} is the more stable oxidation state, oxygen release routinely occurs, forming Ce^{3+} along with an oxygen vacancy to maintain the positive charge.[59] While this redox state exists in the bulk form, the greater surface area to volume ratio associated with NPs means that more reactive species are located at the surface of CNPs, on a mass basis. This allows CNPs to act as both a source and a sink for oxygen. Additionally, CNPs exhibit activity similar to biological enzymes such as phosphatases,[60, 61] oxidases,[62, 63] peroxidases,[64] and ATPases,[65] which is partly the result of their Ce^{3+} and Ce^{4+} surface states. The redox properties (and hence, biological redox activity) of CNPs are highly dependent upon the synthesis method utilized, the implications of which have been thoroughly discussed in recent literature.[66–68]

CNPs are thought to have particular promise for the treatment of neurodegenerative diseases, such as Alzheimer's syndrome (ALZ) and multiple sclerosis (MS).[9] ALZ is thought to be triggered, in part, by increased production of ROS in the mitochondria, which can lead to neuronal cell death.[69] Using CNPs designed to localize to the mitochondria, Kwon and Cha et al.[70] demonstrated that transgenic ALZ mice have increased neuronal cell density compared to CNP-untreated mice. Based on additional experiments, they found that ROS-induced brain inflammation can lead to neuronal loss, but that CNPs reduce this ROS accumulation. From this, they surmise that CNPs reduce inflammation by scavenging ROS,

which thereby reduces neuronal cell death. It is worth noting that these CNPs had a triphenylphosphonium coating, giving them a positive charge which allowed them to accumulate in the mitochondria. CNPs without this coating were distributed randomly in human neuroblastoma cells. Similarly, a mouse MS model treated with CNPs exhibited significantly improved motor functions and reduced brain ROS concentrations compared to control mice.[71] In this study, the CNPs were coated with citrate and ethylenediaminetetraacetic acid (EDTA), which allowed them to maintain stability and osmolality at physiological pH and resist biofouling. The authors argued that this preparation technique is why, unlike other studies, their CNPs did not accumulate in the liver and spleen, but remained in circulation longer.

The ability of CNPs to reduce inflammation may have other medical uses as well. Davan et al.[72] found that CNPs applied to wounds in rats reduced healing time and scarring by increasing collagen production at the wound site. The researchers demonstrated this by surgically removing dorsal skin (2 cm in diameter) from rats and applying a daily mixture of CNPs in paraffin to the wounds. Wound diameter was measured daily and wound tensile strength was measured after 12 d. The researchers found that rats receiving an application of 2 % CNPs had decreased wound sizes after 1 d which continued until 12 d, compared to rats that were untreated, treated with 1 % CNPs, or treated with povidone iodine, a common over-the-counter antiseptic. Wound tissue was removed after the 12 d treatment and tested for tensile strength and collagen-marker (hydroxyproline) content. Excised wound tissue from rats treated with 2 % CNPs had more than double the tensile strength and hydroxyproline content of non-treated rats and approximately 40 % greater tensile strength and hydroxyproline content compared to rats treated with povidone iodine. The researchers attribute the wound healing attributes of CNPs to their ROS scavenging ability, which follows from their dual oxidation states.[72] Similarly, Chigurupati et al.[73] found that CNPs aid in wound healing in mice. They began by examining the impact of CNPs on fibroblast and keratinocyte cell proliferation *in vitro* and found that cell proliferation was significantly increased when incubated with 1 μmol L^{-1} or 10 μmol L^{-1} CNPs compared to controls. They then tested this *in vivo* by excising dorsal tissue (4 mm in diameter) in mice and applying 10 μmol L^{-1} CNPs topically to the wounds daily for 13 d. CNP treated mice had significantly smaller wounds after 1 d and were almost completely healed by 13 d compared to control animals that still had an average wound size of approximately 1.2 mm in diameter.[73] Wound healing was examined by immunostaining tissue sections and examining smooth muscle actin (SMA). SMA was significantly higher in the mice treated with CNPs compared to the control animals at 5 d, 8 d, and 13 d post injury. This suggests that skin cell differentiation into activated myofibroblasts was increased by CNPs; myofibroblasts are beneficial to the wound healing process. Additionally, increased blood vessel density and almost triple the number of leukocytes were found in wound tissue of mice treated with CNPs compared to control, indicating better tissue oxygenation, better debris clearing, and enhanced anti-infection host-control of tissues treated with CNPs.[73]

CNPs have also been assessed for the treatment of cancers due to their antioxidant properties. Cancer cells typically have high levels of ROS, which act in several ways to help maintain the cancerous phenotype, though, for example, signaling and promoting mutations.[74, 75] Alili et al.[76] found that polymer coated CNPs were not toxic to stromal cells

but showed dose dependent toxicity to cultured human melanoma cells *in vitro*. The researchers then used a mouse model to test the effects of CNPs on tumor growth. Mice were implanted with melanoma cells and injected with either a mock treatment or with CNPs at 0.1 mg kg^{-1} every other day for 30 d. Mice receiving the CNP treatment had significantly smaller tumors compared to the mock treatment group. Cell viability assays indicated no impact on normal cells, but a 45 % decrease in viability of melanoma cells after 96 h. CNPs were shown to decrease the invasive capacity of tumor cells by 70 %.[76] Decrease in cell viability and tumor growth seems to be related to pro-oxidant effects in tumor cells with no such effects observed in normal cells. This pro-oxidant effect seems to be related to the higher lactate and H^+ production in cancerous cells compared to non-cancerous cells. When additional H^+ is present, Ce^{3+} reacts with H^+ and $O_2^{\bullet -}$ to produce Ce^{4+} and H_2O_2 according to the following reaction (6):

$$O_2^{\bullet -} + Ce^{3+} + 2H^+ \rightarrow H_2O_2 + Ce^{4+} \quad (6)$$

The researchers investigated this effect by examining the influence of CNPs on apoptosis in fibroblast cells.[77] They found that by incubating fibroblast cells in 150 μmol L^{-1} CNPs for 24 h and then exposing them to H_2O_2, cytochrome c release from mitochondria was drastically reduced compared to non-CNP incubated cells. Additionally, by incubating fibroblasts with CNPs for 5 d, cell proliferation was increased by 180 % compared to control cells. The enhanced growth rate was comparable and slightly higher than that found from other antioxidants such as N-acetyl cysteine (NAC), sodium selenite, or Trolox.[77]

While positive impacts of CNPs seem promising for medical treatments, Yokel et al.[78] warn of the toxicity associated with CNPs and their potential biopersistence in humans. Rats intravenously injected with CNPs at concentrations of 50 mg kg^{-1}, 250 mg kg^{-1}, or 750 mg kg^{-1} showed a dose-dependent increase in Ce concentrations post injection. The highest Ce concentrations were found in the spleen, with decreasing concentrations found in in the liver, blood, and the brain.[79] While the brain showed the lowest concentration of cerium, significantly increased levels of protein bound 4-hydroxy-2-nonenal (HNE) were detected in the hippocampus 20 h post injection, indicating oxidative stress and potential oxidative damage. HNE is highly reactive and can bind proteins to cause functional changes. However, the authors point out that the CNPs were purchased from a commercial vendor and had an unknown surface coating. Any coating on the CNPs may alter their biocompatibility, biodistribution, and biopersistence. Similarly, mice injected with CNPs weekly for 2 to 5 weeks at 0.5 mg kg^{-1} per dose, a much lower dose than the previous study discussed, had the highest Ce concentrations in the spleen, followed next by the liver, lungs, and kidneys.[80] No toxicity was observed in these mice, instead, CNPs acted as an antioxidant in mice treated with CCl_4 to induce liver toxicity via oxidative damage. CNPs worked as well as, if not better than, NAC, a commonly used antioxidant that reduces oxidative stress. However, mice cleared very little of the Ce injected, suggesting biopersistence of these particles. Interestingly, mice given CNPs orally excreted 95 % of them within 24 h. CNPs used by Hirst et al.[80] were coated with carboxyfluorescein, most likely different from the unknown coating used by Yokel et al.[79]

The unique redox surface chemistry of CNPs, which gives them both anti- and pro-oxidant potential, make these NPs attractive for the medical field. Studies suggest that CNP treatment can influence wound healing, reduce neuronal cell death, and arrest the growth of tumor cells in mice through the amplification of ROS. These results, combined with their low toxicity towards wildtype cells, make CNPs a promising modality for nanomedicine applications.

Titanium Oxide Nanomaterials

Titanium dioxide (TiO_2) and its nanoconstituents (TiO_2NMs) have garnered interest towards employment in a plethora of applications in biomedicine. This material has been shown to be an excellent candidate material for incorporation into dentistry (as dental implants) and orthopedics due to factors such as high corrosion and wear resistance, high strength, durability, low density, and especially, biocompatibility.[81–85] In fact, the biocompatibility and bioinertness of this material has been associated with the formation of native oxide layer(s) on the TiO_2 surface when the material comes into contact with air.[86]

TiO_2 NMs show much promise as a PS for PDT cancer treatment applications due to their hydrophilicity and ability to generate electron-hole pairs when exposed to ultraviolet (UV) radiation. These electron-hole pairs, generated after the introduction of TiO_2 into living tissues or cells, can react with surrounding oxygen to form various ROS such as H_2O_2, $^{\bullet}OH$, or $O_2^{\bullet-}$.[87, 88] The effective production of ROS by TiO_2NPs is the main contributing factor in its successful use as cytotoxic reagents in human cervical adenocarcinoma,[89] hepatocarcinoma,[90] non-small cell lung cancer,[91] breast cancer,[92] and leukemia[93] cell lines. In an early study, Cai et al.[89] demonstrated the ROS generating capability (as well as the potential for tumor tissue penetration) of TiO_2NPs as they found that 10 min UV irradiation of TiO_2 particles at 50 μg mL^{-1} was sufficient for complete HeLa cell death. Exposure of TiO_2 treated cells to a 500-W mercury lamp resulted in a dramatic decrease in tumor cell survival (an 80 % reduction in cell survival was found after 5 min of irradiation, while 10 min irradiation resulted in 100 % cell death). Additionally, tumor growth was suppressed in TiO_2 treated cells for up to 30 d. Cytotoxic effects were attributed to the generation of ROS products such as $^{\bullet}OH$ and H_2O_2 on the TiO_2 surface. Later, TiO_2 nanofibers were found to induce not only significant oxidative stress-mediated cytotoxicity at low doses, but also apoptosis in HeLa cells.[94] TiO_2NPs induced the formation of apoptotic features in A549 cells.[90] In the aforementioned study, during comparison of cell morphologies, control cells were found to be large, round, and contained dense microvilli with minor surface protrusions. In contrast, cells exposed to TiO_2NPs were flat with rough cell membrane and thinner microvilli; they contained larger and more numerous protrusions. A decrease in MMP was found for TiO_2NP-exposed A549 cells. Meanwhile, results from the comet assay agreed with similar studies,[95–98] and revealed the dose-dependent DNA damage induced by TiO_2NPs. In each of these studies, the superphotocatalytic properties of TiO_2 materials were employed to investigate and demonstrate anticancer effects.

Conventional drug delivery and administration is often hampered by limitations such as low drug efficacy, poor bioavailability, drug degradation, etc.;[99] however, the photocatalytic properties of TiO_2 and its nanoconstituents make them suitable candidates for single and

multi-drug delivery treatments.[100] Yadav et al. evaluated the biocompatibility of multimodal methoxy PEG (mPEG) TiO_2 nanocoral structures (TiO_2NCs) for chemotherapeutic drug delivery.[101] They assessed the efficiency of these drug loaded TiO_2NCs for tunable drug release of doxorubicin (DOX, mPEG-DOX-TiO_2NCs) in cancer chemotherapy, especially under UV light. *In vitro* toxicity and drug release studies were performed by exposing L929 and MCF-7 (breast cancer cell line) cells to bare TiO_2NCs and mPEG-DOX-TiO_2NCs and the level of ROS production in MCF-7 cells was measured using the 5-(and-6)-chloromethyl-2,7-dichloro-dihydrofluorescein diacetate-acetyl ester (H_2DCFDA) assay. Due to the uniquely high-surface area of the TiO_2NC architecture, drug loaded TiO_2NCs acted as not only as efficient drug carriers, but also mediated cancer cell death under light activation. mPEG-TiO_2NCs were proven to facilitate higher DOX uptake and delivery into cells, and enhanced targeting of cancers cells, thus activating apoptosis (evidenced by cell shrinkage, cell extensions, and an increase in the number of floating cells) through the generation of excess ROS under UV illumination. ROS generation was attributed to the electron-hole pairs created by TiO_2NCs under UV illumination. MCF-7 cells exposed to UV, bare TiO_2NCs, and mPEG- DOX-TiO_2NCs and after 20 min of irradiation displayed 71 %, 51 %, and 16 % cell viability, respectively indicating the anticancer effect of mPEG-TiO_2NCs due to the production of free radicals such as $^{\bullet}OH$ and $O_2^{\bullet-}$.

Although TiO_2NPs have been shown to be bioinert, evidence on the cytotoxic effects of smaller-sized particles has been demonstrated in the form of pulmonary inflammation, emphysema, and epithelial cell apoptosis.[102–104] Additionally, TiO_2NP exposure *in vitro* has resulted in damage to lipid, protein, and DNA, as well as cytoplasmic membrane rupture.[104–106] In most cases, cytotoxic effects were a result of increased ROS generation after exposure. Zhu et al.[107] investigated the influence of oncongenic transformation and apoptotic signaling pathway on cellular responses to TiO_2NP-exposure in isogenic wild-type and apoptosis-resistant ($Bak^{-/-}Bax^{-/-}$) cell lines. Two pairs of wildtype (untransformed) mouse embryonic fibroblasts and their isogenic counterparts (one pair of cells expressed all Bcl-2 proteins and another pair was deficient in expression of two key proapoptopic Bcl-2 proteins) were exposed to increasing concentrations of TiO_2NPs (type P25) for 24 h. After 24 h, TiO_2NPs entered cells via endocytosis and were visualized as clusters of TiO_2NPs sequestered within vacuoles inside the cell. Some of the particles were localized to the cytoplasm (which could have been resultant of lysosomal membrane rupture). They observed a dose-dependent decrease in the viability of all four cell lines tested. They provided evidence that TiO_2NPs preferentially induce tumor cell death through a lysosome-mediated pathway, and noted that lysosomal membrane permeability and necrosis resulted from severe oxidative stress. When comparing responses for transformed and untransformed cells, they also found that transformed cells were more sensitive to TiO_2NPs. They regarded this preferential killing of transformed cells by TiO_2NPs as a potential area of exploitation for cancer therapy.

While toxic effects are not ideal in the field of nanotechnology, exploitation of the photocatalytic properties of TiO_2 led to the demonstration of TiO_2-mediated cytotoxicity in cancer research. Lagopati et al.[92] investigated the feasibility of employing TiO_2 as an anticancer agent in the presence of ultraviolet light. They hypothesized that crystallinity would impact oxidant generation, and therefore explored the effect of the particle crystal

phase of TiO_2 dispersions using two breast epithelium cancer cell lines: MDA-MB-468 and MCF-7. A reduced cell viability of both cell lines was exhibited with both 100 % anatase TiO_2NPs and TiO_2 P25 (anatase-rutile mixture [75 %: 25 %]) at increasing exposure concentrations. This decrease in viability was compounded under UVA irradiation. Photoexcited 100 % anatase TiO_2NPs induced greater apoptosis and DNA fragmentation. Overall, they found that the highly malignant MDA-MB-468 cells were more susceptible to UVA-activated TiO_2NP and induced cell death as compared to MCF-7 cells, especially in the case of treatment with the 100 % anatase NPs. This cytotoxic effect agreed with the conclusions of Sayes et al.,[105] who found that anatase phase TiO_2NPs generated more ROS in human dermal fibroblasts or A549 cells. The mechanism of TiO_2NP cytotoxicity involved an increase in Bax-expression (one of the proteins integral in the cell apoptosis pathway) which was a novel finding about the exposure effects of pure anatase TiO_2 *versus* anatase-rutile mixtures.

In conclusion, properties and characteristics, such as the ones highlighted here and as well as many more, have allowed for the innovative implementation TiO_2NMs into drugs, treatments, and devices in the field of nanomedicine. Their unique ability to serve as vehicles and carriers in PDT have garnered advances in varying cancer treatments and improved therapeutic delivery, promoting cellular responses. Additionally, their use in cancer therapy is directly resultant of their ability to foster ROS generation. Future advances in nanomedicine will more than likely build off the many ways the properties TiO_2NMs can be exploited.

Gold Nanomaterials

The unique properties of gold-based nanomaterials (AuNMs), such as their optical properties biocompatibility, high stability, and multifunctionality, make them highly attractive for many applications in nanomedicine.[108–110] These applications include, but are not limited to, electrochemical sensing, cell and tissue imaging, targeted therapeutic delivery, and photo-induced cancer treatments.[109–115] Moreover, because of their multifunctionality, AuNMs have been used recently as theranostics probes to simultaneously target, diagnose, deliver a therapeutic function, and monitor response to therapy in highly specific single clinical procedures.[110, 111]

While gold nanoparticles (AuNPs) generally cannot be considered redox active, the presence of AuNPs in biological systems induces other interactions that may cause some biological redox responses. AuNPs are an ideal platform for electrochemical biosensors because they can act as redox catalysts, enabling enhanced electron transfer for a wide range of electroactive biological species (mainly redox proteins) and avoiding the use of electron transfer mediators.[112, 113, 116–118] Furthermore, their higher surface area provides stable immobilization of proteins, retaining their bioactivity and allowing for increased protein loading, which provides more sensitivity than flat gold surfaces.[113, 116, 119, 120] The main research areas for the application of AuNPs in electrochemical sensing involve the direct electrochemistry of redox proteins (mainly enzymes), electrochemical genosensors (DNA), aptamer sensors and immunosensors for the determination of clinically significant biomarkers relevant to the diagnosis and/or monitoring of human diseases (e.g.

cancer).[117, 121–123] Particularly, AuNPs have been demonstrated to be useful interfaces for the electrocatalysis of redox processes with molecules (NADH, cholesterol, glucose, etc.) pertinent to many significant biochemical reactions.[118, 124, 125] Ciganda et al. demonstrated that AuNPs can also act as electron reservoir redox catalysts for 4-nitrophenol reduction (4-nitophenol is an additive used in manufactured drugs, fungicides, insecticides that causes cyanosis, headaches, nausea, etc. in humans), exhibiting a strong stereoelectronic ligand influence.[126] AuNPs have also been involved in the sensitive detection and quantification of ROS such as H_2O_2 and $O_2^{\bullet-}$.[113, 121–123]

The role of AuNPs in ROS generation and DNA damage by oxidative stress has been significantly studied in recent years. AuNPs induce lipid peroxidation, reduce the levels of glutathione peroxidase and significantly increase the levels of 8-hydroxydeoxyguanosine, that indicate DNA damage by oxidative stress in rat brain.[127] Similarly, AuNPs induce oxidative damage through ROS in lung fibroblasts *in vitro*, which is one source of DNA damage.[128] Furthermore, in the model organism *Drosophila melanogaster*, significant concentration-dependent and size-independent ROS generation was found, which precipitated DNA damage and cell death after ingestion of AuNPs (5 nm to 80 nm size range).[129] It was also reported that AuNPs may or may not induce oxidative stress in different species of marine bivalves.[130, 131] Intracellular AuNPs can also promote the generation of ROS, leading to ROS-induced DNA damage.[132]

Nethi et al.[133] proposed a novel eco-friendly approach of synthesizing AuNPs by utilizing *Hamelia patens* (HP) leaf extract as a stabilizing/capping agent, which also exhibited an excellent pro-angiogenic activity in human umbilical vein endothelial cells. The beneficial ability of the bioconjugated AuNPs (HP-AuNPs) to make new blood vessels without promoting cancer cell proliferation *in vitro*, was corroborated in a chicken embryo angiogenesis *in vivo* assay. This finding opens the door to potential applications of HP-AuNPs in alternative treatment strategies for wound healing and cardiovascular and ischemic diseases. On the contrary, in both assays an antiangiogenic activity was observed for PEG-coated AuNPs (PEG-AuNPs), indicating a crucial role of the coating in the biological response. It has been reported that ROS, including H_2O_2 and $O_2^{\bullet-}$, are established as major redox signaling molecules in physiological angiogenesis. Consequently, the detection of ROS in endothelial cells after exposure to HP-AuNPs was carried out by fluorescence microscopy. The results revealed an enhanced generation of H_2O_2 and $O_2^{\bullet-}$ for cells treated with HP-AuNPs compared to PEG-AuNPs, suggesting that the controlled ROS generation and consequent redox signaling might be the probable mechanism of HP-AuNPs induced angiogenesis. Additionally, HP-AuNPs also enhanced phosphorylation of Protein Kinase B (involved in critical signal transduction of various cellular processes) when compared to PEG-AuNPs.

Considering the beneficial use of ROS in PDT for cancer, Khaing Oo et al.[134] evaluated the enhancement of ROS formation by AuNPs. Generally, the AuNP PS conjugates result in effective energy or electron transfer between the photoactive dye and AuNP, leading to a more effective photodynamic effect. In this case, the size-dependent enhancement of ROS formation enabled by AuNPs with different diameters (19 nm, 66 nm, and 106 nm) conjugated to a PS, protoporphyrin IX (PpIX), was investigated. They demonstrated that the

ROS formation was enhanced proportional to AuNP size after irradiation of PpIX. This effect was due to the localized electromagnetic field of the surface plasmon resonance for illuminated AuNPs. Concretely, photosensitized 106 nm diameter AuNPs enhanced the ROS ratio 5 and 3 times higher than photosensitized 19 nm AuNPs and 66 nm AuNPs, respectively. In a subsequent *in vitro* study, AuNPs were reported to act as cytotoxic agents by inducing ROS in the MDA-MB-231 cancer cell line, which lead to significant cell destruction.[134] The authors also found that the intracellular ROS formation enabled by PpIX-AuNP conjugates was also proportional to the size of Au NPs. This ROS enhancement greatly depended on the cellular uptake of AuNPs. In fact, when intracellular $^1O_2$ levels were monitored as a readout of AuNP uptake, the greatest ROS enhancement was observed from 66 nm AuNP-treated cells. Although more than 50 % of breast cancer cell destruction was obtained for all PpIX-AuNPs, the 66 nm Au NPs yielded the highest destruction rate (60.4 %), consistent with the highest cellular uptake and highest ROS formation. These findings clearly shed new light on AuNP-assisted PDT, demonstrating that the size-dependent ROS generation, cellular uptake, and the complexity of the cellular environment all contribute to the overall cellular PDT efficacy.

Di Bucchianico et al.[135] investigated the potential *in vitro* cytotoxicity and genotoxicity mechanisms exerted by differently sized AuNPs. The authors used human primary lymphocytes and murine macrophages (Raw264.7) that were exposed to different mass concentrations and number densities of spherical citrate-coated AuNPs of 5 nm and 15 nm diameter. Results indicated that both AuNP sizes significantly decreased the cell viability of these two cell models by 20 % to 30 % following exposure to 10 μg mL^{-1} over 24 h. Exposure induced apoptosis, aneuploidogenic effects, and DNA oxidation. Moreover, they showed a size-independent correlation between cytotoxicity and their tested mass concentration or absolute number. However, it was clearly established that genotoxic effects were more severe for larger AuNPs. Overall, they concluded that apoptosis, aneuploidy, and both DNA damage and oxidation play a pivotal role in the cytotoxicity and genotoxicity elicited by differently sized AuNPs.

Gold nanoclusters (AuNCs) are a particularly interesting subset of gold NMs, with unique properties distinct from AuNPs. AuNCs are ultra-small gold particles, with particle diameters smaller than 2 nm, which are typically composed of a few to about 100 gold atoms. AuNCs exhibit molecule-like properties such as discrete electronic states and size-dependent fluorescence, and bridge the gap between isolated metal atoms and plasmonic metal NPs.[136–138]. Due to their excellent fluorescence properties, photostability, good biocompatibility, and enhanced catalytic activity,[139–143] AuNCs have been recently used in the field of bioanalysis,[142, 144] bioimaging,[142, 145] multifunctional control drug release,[143, 146] theranostics and cancer therapy.[143, 144]

Unlike AuNPs, AuNCs can be considered redox active NMs because of the quantum size effect that leads to discrete electron transition energy levels. For example, hexanethiol-capped AuNCs (Au_{147}, d = 1.62 nm) display 15 redox states at room temperature,[147] demonstrating that AuNCs can possess molecule-like redox properties.[148] These unique redox properties can be tuned effectively by external ligands, magnetic fields, electrolyte ions, and by controlling the core size.[149–153] Moreover, the reversible charge-state

conversion of AuNCs indicates that they can be utilized in catalytic oxidation or reduction reactions.[154] An overview of representative examples of AuNCs as redox catalysts, including the reduction of CO_2 to CO, the reduction of O_2, as well as the oxidation of styrene, SO_2, cyclohexane, and benzyl alcohol, can be found elsewhere. Although the electrochemical properties of the AuNCs have yet to be adequately investigated, an electrochemistry approach is well suited to the design and development of commercial biosensors. Recently, AuNCs have been reported to act as an electron transfer bridge in the electrochemical sensing of different biomolecules such as glucose, ascorbic acid, uric acid, dopamine, bilirubin, and H_2O_2.[155–158] A new finding has demonstrated that the strong fluorescent signal of AuNCs can be sensitively and selectively quenched by ROS, fostering a very promising application field for AuNCs as probes for ROS detection. This new role of AuNCs as analytical tools in the oxidative stress field has been recently reviewed.[144] An illustrative example, based on this approach, is the quantitative determination of H_2O_2 over a wide dynamic range (100 nmol L^{-1} to 1.0 mmol L^{-1}) with a limit of detection of 30 nmol L^{-1}, comparable to other optical H_2O_2 sensors.[159] Furthermore, the use of AuNC-protein conjugates to selectively monitor endogenous H_2O_2 production in live cells by fluorescence quenching has been very recently reported.[160]

Lei et al.[161] investigated the capabilities of AuNCs decorated with polypeptide/DNA complexes as versatile gene delivery platforms for dual-responsive near-infrared light (NIR) and redox activity during gene transfection. Photo-induced endosome/lysosome disruption has recently opened a new avenue into the design of gene carriers based on the generation of low amounts of ROS after mild light irradiation. Irradiation-induced ROS enables selective control over endosome/lysosome escape without destroying the loaded gene and also avoiding cell death. AuNCs exhibit superior features versus previous photo-controlled delivery systems due to their ROS generation capability, NIR excitation wavelength (808 nm), greater hydrophilicity, and easier synthesis and modification processes. In this study, a polypeptide/DNA complex loaded with the desired gene was decorated with a captopril-stabilized Au_{25} nanocluster for its ability to be internalized via endocytosis and generate ROS to accelerate endosome/lysosome escape under mild NIR-irradiation. After glutathione-induced disulfide bond breakage in the cytoplasm, nuclear translocation results in enhanced gene transfection. Followed by glutathione induced disulfide bond breakage in the cytoplasm, the nuclear translocation was facilitated resulting in an enhanced gene transfection. To avoid the potential cytotoxicity associated with ROS generation by AuNCs, AuNC concentrations and NIR light exposure conditions were optimized to guarantee biocompability of AuNCs and to prevent cell death. Furthermore, this work successfully demonstrated the selective destruction of acidic organelles through NIR irradiation fluence-modulation. It is expected that this very promising versatile gene delivery platform, based on the use of AuNCs as the ROS generator, may be further exploited in new photo-induced gene delivery strategies with spatiotemporal control.

In summary, while AuNPs do not impart a direct redox interaction on biologics, AuNCs can exhibit molecule-like redox properties. Both gold-based NMs play an important role in the electrochemical sensing of redox biomolecules. As described earlier, both AuNPs and AuNCs can also participate in the generation of ROS. Overall, their outstanding properties, combined with their good biocompatibility and typical low toxicity, make gold-based NMs

promising modalities for nanomedical applications. Advances in the use of gold-based NMs for nanomedicine applications need to be followed by parallel bio-distribution and toxicity studies with maximum care and accuracy to guarantee their success.[114, 115, 129, 162–164]

Silver Nanoparticles

Recently, silver NPs (AgNPs) have been used for a variety of applications in medicine and in commercial products due to their bactericidal properties.[165–169] AgNPs have been incorporated into bandage formulations to reduce inflammation and promote wound healing [170]. They are used in a variety of medical procedures and devices to reduce the likelihood of infection, such as incorporation into bone cement[171] and catheters.[172] Commercially they are used in cosmetics,[173] home appliances (e.g., air and water filtration systems),[174, 175] and textiles.[176] AgNPs also have unique plasmonic properties, which have been exploited for use in contrast agents for bioimaging, including for photoacoustic imaging of cancer cells.[177]

On a cellular level, AgNPs are internalized through endocytosis pathways and translocated to target organelles (e.g., mitochondria, nucleus) where they can activate genotoxic and cytotoxic pathways and ultimately lead to cell death.[178] The two putative mechanisms by which AgNPs contribute to cell death are: 1) through dissolution and subsequent release of bioactive silver ions (Ag^+)[178, 179] and/or 2) through the generation of ROS by either Ag^+ or AgNPs.[167, 178, 180] Several studies have sought to clarify these toxicity mechanisms both from the perspective of how they could have potentially harmful effects or how the cell death pathways could be used beneficially. For example, research has been conducted from a human exposure standpoint by monitoring cytotoxicity to liver cells after their accumulation in this organ,[181, 182] or by monitoring lung cells in order to understand the potential adverse effects of inhalation exposure.[183, 184] Other studies have evaluated AgNP cytotoxicity mechanisms in fibroblasts and macrophages to understand the use of AgNPs to improve wound dressings,[185] or in bacteria and cancer cells to understand the role AgNPs could play in reducing infection and disease.[165–169, 186, 187]

Cell viability in the presence of AgNPs is largely dictated by redox mechanisms. Translocation of AgNPs to the mitochondria, redox active organelles in the cell, is thought to result in the formation of ROS. In many cell lines, ROS cause mitochondrial disruption, oxidative stress, DNA damage, and eventual cell death via apoptosis.[166, 167, 181–185] This redox activity is evidenced in a number of studies; some have shown that low concentrations of AgNPs trigger increases in antioxidants like GSH or SOD and decreases in lipid peroxidation,[181] while others note decreases in antioxidant levels in the presence of AgNPs. Specifically, in human liver cells, decreases in GSH were observed along with decreases in the protein expression of the catalytically active subunits of two GSH-synthesizing enzymes. These responses were accompanied by mitochondrial membrane disruption through down-regulation of Bcl-2 protein and concomitant up-regulation of Bax protein.[182] Bcl-2 prevents opening of the mitochondrial membrane, while Bax accelerates its opening. The combined effect of their respective down-regulation and up-regulation was shown to induce the release of cytochrome C into the cytosol, which triggered the activation of caspase 9 and caspase 3 leading to cell death via apoptosis.[182] Herein, the redox activity of AgNPs is described first

in the context of its effects relating to cell death, and subsequently in its utilization as a targeted therapy for cancerous cells.

Many of the studies conducted to understand the mechanism through which AgNPs are genotoxic or cytotoxic were performed *in vitro*. To corroborate these studies, work conducted *in vivo* indicates that ROS-dependent pathways play an important role in the effects of AgNPs. In one study, Swiss albino mice were analyzed 24 h and 72 h after intraperitoneal administration of varying doses of AgNPs (26 mg kg^{-1}, 52 mg kg^{-1}, and 78 mg kg^{-1}).[188] A dose- and time-dependent increase in DNA damage was observed in liver cells and lymphocytes. Further, staining of liver tissue samples revealed dose- and time-dependent apoptosis of liver cells and necrosis in some regions.[188] Similarly, other work has demonstrated increases in markers of oxidative stress after treating Swiss albino mice with varying doses of AgNPs over a period of 14 successive days.[189] Depletion of GSH was observed in the blood indicating an increase in blood ROS levels, while the effect of AgNPs on tissue ROS levels varied depending on location. A significant increase in a DNA damage marker was also observed in the urine.[189] These *in vivo* studies have important implications for the use of AgNPs for medicinal purposes, and since the most deleterious effects were observed for the highest dose of AgNPs administered in each study, these studies highlight the importance of dosing in potentially mitigating these adverse effects.

The same mechanisms by which AgNPs may induce harmful effects can be used for the development of AgNPs as therapeutic agents. PVP-coated AgNPs have shown increased cytotoxic effects against six cell lines from patients with acute myeloid leukemia (AML) relative to cells from healthy patients.[186] Cytotoxicity was determined to result from the generation of ROS, which led to changes in the MMP, DNA damage, and cell death via apoptosis. ROS generation was confirmed through a fluorescence assay and through the independent introduction of two antioxidants, vitamin C and NAC. Interestingly, both vitamin C and NAC attenuated AgNP-induced ROS generation, but only NAC prevented losses of MMP, induction of DNA damage, and cellular apoptosis. It was proposed that NAC can act as a Ag^{+} scavenger, which would suggest that losses of MMP, DNA damage, and apoptosis are, at least in part, due to the presence of ionic silver.[186]

In all six AML cell lines, cell viability decreased in a dose-dependent manner for three different sizes of AgNPs, with no significant difference in IC_{50} for AML and healthy cells ($IC_{50} \approx 4$ μg mL^{-1}). However, at low AgNP concentrations (≈ 1 μg mL^{-1} to 2 μg mL^{-1}), cell viability decreased more significantly for AML cells than for healthy cells indicating increased cytotoxicity of AgNPs to AML cells at low dosage.[186] The differential dose-response at low AgNP concentration is significant when taken together with other research exploring the use of biocompatible nanocarriers (NCs) as a means of delivering AgNPs to cancer cells with high efficiency and efficacy.[187] Specifically, AgNP-chitosan nanocarriers (Ag-CS NC) have shown increased cytotoxicity for human colon cancer cells with an IC_{50} value of 0.33 μg mL^{-1}. Toxicity proceeds through an apoptotic pathway triggered by mitochondrial dysfunction and ROS production. Additional increases in the toxic nature of AgNPs towards cancer cells when incorporated into a nanocarrier system coupled with the ability of the nanocarrier to be modified for improved biocompatibility and targeted delivery potentiates the use of AgNPs as cancer therapies.[187]

In summary, AgNPs are promising platforms for the development of novel therapies. *In vitro* and *in vivo* studies support a mechanism whereby AgNPs induce apoptotic cell death through ROS-mediated pathways. While a general understanding of the mechanism of action of AgNPs can be extrapolated from the studies described here, it's important to note that cellular response is specific to the AgNP size, surface coating, and concentration, as well as the cell line used. Thus, the pathways through which AgNPs may produce impacts are highly specific to the system, necessitating additional systematic, well-controlled studies. With careful tuning of AgNP properties, their potential for use as direct therapeutic agents or as nanocarriers for other small molecules may be realized.

Selenium Nanoparticles

A nonmetal with physicochemical properties between sulfur (S) and tellurium (Te), selenium (Se) is present in several proteins that play a critical role in maintaining cellular redox homeostasis (glutathione peroxidase, thioredoxin reductase) and thyroid hormone production (iodothyronine deiodinase).[190, 191] Various inorganic, organic and amino-acid Se derivatives have been found to exhibit biological activity, primarily through antioxidant and pro-oxidant mechanisms.[192–195] Epidemiological studies have identified Se compounds as being effective in the prevention and treatment of diseases where oxidative stress is implicated, namely cancer, cardiovascular, and neurodegenerative diseases. Due to the elevated concentration of both ROS and antioxidants in cancer cells, redox state modulation is a possible target for anticancer agents.[196, 197] Se has lower electronegativity making its compounds more potent reducing agents than S analogues (e.g. $E_{Secysteine} = -0.38$ V vs $E_{Cys/Cystine} = -0.23$ V[196]). *In vivo*, Se can be reduced by thiol compounds or oxidized by oxygen with both reactions producing ROS that trigger apoptosis. Lung, prostate, cervical, and colon cell culture experiments have shown that selenite (SeO_3^{2-}) acts as a cytotoxic pro-oxidant in cancer cells.[194] However, *in vivo* studies have also revealed that SeO_3^{2-}administration is toxic if administered at doses outside of the narrow therapeutic window.[197]

The latest research on anticancer properties of Se compounds demonstrated that concentration, chemical speciation, redox potential, and treatment model are all critical determinants of its therapeutic activity.[198, 199] If administered in low doses, inorganic Se controls ROS concentration in wildtype cells while in dysplastic cells Se will turn into a pro-oxidant, which highlights the higher sensitivity of an abnormal cellular phenotype to Se supplementation.[200,201] In higher doses, SeO_3^{2-} selectively causes apoptosis in malignant cells, while sparing the benign cells.[202] Such non-linearity in biological activity led to the hypothesis that the Se dose-response curve may have a U shape, which suggests a critical role for Se cellular uptake and metabolism control in therapeutic strategies.[194, 203] Besides direct anti- and pro-oxidant based activities, Se compounds are capable of binding copper and iron and thus averting oxidative damage by ROS generated via a Fenton reaction.[204] Evidence also suggests that the increased expression of Se containing thioredoxin protects against cardiovascular diseases.[205]

Recent advances in nanotechnology offer a wide range of novel Se structures with larger degree of control over their biological activity and toxicity compared to inorganic and

organic compounds.[206–210] Control of Se nanoparticle (SeNP) size, shape, morphology, and surface structure are the useful properties for tuning their therapeutic efficacy and biocompatibility. Elemental Se becomes biologically active when as the red-allotrope NP,[211–213] which is less toxic than other forms (SeO_3^{2-}, selenomethionine, methylselenocysteine). SeNPs can be prepared by a large variety of physicochemical methods (reviewed in[214]) although so-called green methods are preferred for bio-medical applications. Often chemical reduction of SeO_3^{2-} and/or selenate (SeO_4^{2-}) by non-protein thiols in microorganisms,[215, 216] or GSH in the presence of bovine serum albumin produce red SeNPs.[211] Promising antitumor activity and low toxicity of bare SeNPs to healthy cells was achieved for several cancer cell lines.[216–220] NP surface functionalization with various ligands serves to prevent particle aggregation, modulate cellular uptake and stability, and even selectively target cancer cells through binding with overexpressed membrane receptors. Se particles with surface ligands containing polysaccharides,[221, 222] sialic acid,[223] chitosan,[224] folate,[225] transferrin,[226] undecanol,[227] siRNA,[228] poly-ethylene-glycol,[229] and porous silica[230] are among recently tested NPs for anticancer application.

A growing trend is to combine Se with other antitumor agents, antibacterial agents, or different material-based NPs to generate molecularly-tunable anticancer or antibacterial nano-platforms.[209, 210, 230–235] Mary et al.[229] describe a drug-delivery system designed by attaching a crocin, an active product of saffron, to PEG-modified SeNPs. These constructs significantly inhibited tumor growth in a nude mice model. At up to 10 % loading, crocin inhibited A549 cell growth in a time and dose dependent manner, while showing no effect on L-132 cell growth. Moreover, the combination of both crocin and SeNPs was demonstrated to have strong synergy in inhibiting cancer cell growth. The authors also detected mitochondrial membrane depolarization in treated cancer cells. Depolarization is considered to be an initial step in the apoptosis cascade.[229] A synergistic effect of the anticancer drug doxorubicin with ultra-small SeNPs was also highlighted by Liu et al.[230] via 55 nm porous silica-Se nanospheres impregnated with doxorubicin. Their nano-platform showed less than 10 % inhibition of wildtype cell up to 400 μg mL^{-1}, while demonstrating cytotoxicity (viability less than 50 %) to HeLa cells in a range from 50 μg mL^{-1} to 150 μg mL^{-1}. In both studies, a pH-sensitive drug release strategy was exploited to discriminate between wildtype and cancerous cells. In addition to lower pH, tumor cells also possess a higher cytosolic reduction potential;[190] this distinction was exploited by Zhang et al.[231] who developed a “smart nanocarrier” with built-in redox dependent stability. They incorporated a diselenide-containing fluorescent molecule with the antitumor drug paclitaxel (PTX) into a 157 nm diameter particle using a nano-precipitation method. Particle redox sensitivity was tested by incubating with GSH, which is the principal cytosolic redox buffer. When exposed to GSH, the diselenide bonds were reduced to SeH resulting in time-dependent particle disintegration. Cytotoxicity of their NPs against tumor (HeLa and MCF-7) and wildtype (BEAS-2B and L929) cells was evaluated using the MTT assay. It was reported that 60 % to 75 % of cancer cells were killed at 5 μg mL^{-1} PTX loading compared to 20 % to 25 % of the wildtype cells. Combining two or more active compounds in Se containing nano-platforms opens new pathways for synergistic treatment of cancer, while also boosting selectivity and lowering toxicity to wildtype cells.

The primary research focus in SeNP biomedical applications is for cancer, yet other ailments are also addressed. Kumar et al.[236] recently demonstrated that the progression of diabetic nephropathy in rats was significantly slowed after administration of SeNPs. Diabetes was induced in rats by injecting streptozocin and nephropathy was evaluated by measurements of blood nitrogen, creatinine, albumin, fibronectin and collagen. Remarkably, SeNP also activated cyto-protective (HSP70) and longevity-related (SIRT1) proteins; oxidative stress quenching also modulated apoptotic proteins, Bax and Bcl-2. Towards a potential ALZ treatment, Zhang et al.[237] designed nano-particles with an anti-amyloid agent, Epigallocatechin-3-gallate (EGCG), and selenoproteins to effectively convert protein fibrils into non-toxic aggregates. The authors synthesized SeNPs terminated with a neuro-affinity peptide, TET-1, to significantly enhance the cellular uptake of the EGCG into PC12 cells. Disruption of the interaction between metal ions and peptides is a promising new therapeutic strategy for ALZ treatment. Yang et al.[238] modified Se/ruthenium (Ru) NPs with L-cysteine to create amyloid binding units. These particles were found to suppress a Zn^{2+}-amyloid ROS generation mechanism, which resulted in neurotoxicity in PC12 cells. The spherical NPs with varying surface charge were shown to significantly decrease the volume of intracellular peptide aggregates. The presence of Ru in these NPs also retarded the functioning of random coiling, sheet formation and disturbed the alpha helical structures of the amyloids.

In summary, notable advancements in recent years have been made towards developing SeNP applications in the biomedical field. Many recent SeNP constructs have been shown to possess efficient and selective therapeutic and diagnostic potential. Although some mechanistic aspects of Se bioactivity are still unknown, its unique redox properties, versatile chemistry and natural biocompatibility are the main drivers for this growing field. Ongoing challenges towards the wider acceptance of SeNP-based therapies in clinical practice are improving dosing accuracy, potential toxic limits, and better understanding how SeNPs are metabolized by the body.

Graphene and its Derivatives

Monolayer graphene is one of the many nanostructured allotropes of carbon (fullerenes, CNTs, carbon dots, etc.) that is the subject of extensive research efforts in diverse areas of nanomedicine and biology. Initially isolated via the mechanical exfoliation of graphite in 2004,[239] graphene is essentially a 2D monolayer sheet of sp^2-hybridized carbon atoms that possesses extraordinary chemical and physical properties such as its inherently high electrical conductivity. Graphene is especially noted for its remarkable mechanical strength,[240] superior electronic properties,[241, 242] and high thermal conductivity.[243] As graphene is a monolayer of carbon atoms, all of its atoms are directly on its surface and thus graphene has the potential to interact with biomolecules directly. In addition, the surface of graphene consists of delocalized π electrons which can be effectively utilized for loading aromatic drugs, such as the drugs commonly utilized in cancer chemotherapy. Due to its 2D planar nature, graphene is estimated to have the largest specific surface area ($\approx 2600\ m^2\ g^{-1}$) in comparison to most other NMs utilized in biological applications.[244] The large specific surface area, along with the availability of surface atoms and the presence of delocalized π electrons, enables graphene to be an effective nano carrier in which both sides of the 2D planar sheet can be functionalized with a variety of drug molecules, targeting ligands and

imaging agents. However, the strongly hydrophobic nature of graphene prevents it from being widely utilized in nanomedicine applications due its inherent instability and tendency to aggregate in aqueous and physiological solutions. Hence most research and applications of graphene in nanomedicine focus on the utility of other graphene derivatives such as graphene oxide (GO) and reduced graphene oxide (rGO) because these forms have enhanced solubility and dispersion properties in aqueous and physiological solutions in comparison to graphene.[245, 246]

Current research on the potential use of GO and rGO and their hybrids and derivatives in nanomedicine research is expansive and continuing to grow at a rapid pace. GO and rGO find application in 1) drug/gene delivery, 2) phototherapy, 3) biomedical imaging, 4) tissue engineering, 5) biosensing and in 6) regenerative medicine.[245–256] GO/rGO can function to directly oxidize or reduce analytes of clinical or medical importance. The main examples of a direct redox functionality for GO/rGO are, of course, the capacity of these materials to act as peroxidase-like mimetics[257] or as antibacterial/antimicrobial agents.[258] Next generation graphene derivatives, such as graphene quantum dots (GQDs) have also been shown to be unique antibacterial agents. Most recently, GQDs but have been shown to function as direct and efficient PSs for use in PDT applications.[259]

Peroxidases, such as horseradish peroxidase (HRP), are oxidoreductase enzymes that scavenge H_2O_2. HRP works by catalyzing the reduction of H_2O_2 to H_2O by transferring two electrons from a substrate that acts as an electron donor.[260] A typical substrate, such as 3,3,5,5-tetramethylbenzidine (TMB), is oxidized and converted into a blue-colored compound which can be quantified through spectrophotometric detection. The amount of oxidized TMB is directly correlated to the amount of H_2O_2 present in the system. Recently, Song and coworkers[257] demonstrated that carboxylated GO (COOH-GO) could function as an efficient peroxidase-like mimetic for the quantitative determination of H_2O_2. The authors substituted their synthesized COOH-GO for HRP and showed that the peroxidase substrate, TMB, could be efficiently oxidized to a blue compound in solution. In subsequent experiments, the authors showed that the peroxidase-mimetic activity of COOH-GO could be utilized to determine human blood glucose levels by using the glucose oxidase enzyme to convert glucose to H_2O_2 and then using the COOH-GO/TMB redox reaction to measure the generated H_2O_2. This work illustrates the potential use of COOH-GO peroxidase-like catalytic activity for the measurement of glucose levels in diabetic patients. More recent studies by Wang and coworkers[261] showed that few-layer-graphene (FLG), exfoliated from graphite, exhibits peroxidase-like catalytic activity for the detection of H_2O_2 that is approximately 45 times greater than GO and 4 times greater than rGO. This remarkably high peroxidase-like activity of FLG was attributed to the higher conductivity in FLG in comparison to the conductivity in GO and rGO; FLG was directly exfoliated from graphite and it has significantly fewer defect sites than GO and rGO and consequently higher conductivity. A complete review of GO and GO-hybrid peroxidase-like mimetics utilized in biological applications has been recently published.[262]

The understanding and characterization of pathogenic bacteria and complex microbial communities (microbiomes) is rapidly evolving, yet “superbugs” which demonstrate remarkable resistance to common antibiotic treatments threaten to create a global health

crisis.[263] Novel nanomedicine strategies that are based on the utilization of NMs such as GO and GO hybrids to combat multidrug resistant bacteria are gaining traction in this arena.[264] There exists three main mechanisms by which GO has been postulated and sometimes demonstrated to effect the destruction of bacteria: 1) direct physical interaction via puncturing of the bacterial membrane and subsequent leakage of bacterial contents;[265–269] 2) direct physical interaction via wrapping of GO around bacteria leading to nutrient deprivation and/or 3) induction of oxidative stress/damage to bacterial membranes via ROS generation.[267, 270] These putative mechanisms are controversial as some studies show supportive data,[258, 268] while other studies show conflicting effects or even that GO remarkably enhances bacterial growth.[264, 271]

Currently, the most widely accepted mechanism for the bacteria-killing ability of GO and its derivatives is based on their propensity to induce oxidative stress. The pathways by which GO can damage bacterial membranes can be either ROS-independent or ROS-dependent.[264, 267, 272] The ROS-independent pathway is exemplified by bacterial inactivation without the direct involvement of ROS, but instead, bacterial inactivation depends upon the discrete inactivation of intracellular biomolecules that are critical for bacterial survival.[267, 273] For example, Liu and coworkers[267] showed that four different types of graphene-based materials (graphite, graphite oxide, GO and rGO) were all able to inactivate *E. coli* to varying degrees due to a combination of membrane damage and oxidative stress damage. However, none of the materials produced detectable acellular ROS levels in the form of $O_2^{\bullet-}$ (as measured by an XTT assay), but all the materials could oxidize acellular GSH to glutathione disulfide (GSSG). Interestingly, the rGO material induced the greatest oxidation of GSH, but GO had the strongest effects on *E. coli* inactivation. The authors hypothesized that since rGO is a much better electrical conductor than the other graphene materials utilized in the study, it was better able to mediate electron transfer from GSH to the external environment. GO, on the other hand, had the advantage of small size and better dispersibility and was thus able to encounter the bacteria and induce membrane stress.

ROS-dependent pathways for bacterial inactivation by GO and its derivatives are based upon having a proportionally high density of defect sites on the basal planes and edges of GO. Several investigators have postulated that molecular O_2 adsorbs to these defect sites and undergoes reduction (mediated by electron transfer) in the presence of antioxidant small molecules and enzymes to ROS.[274, 275] These ROS can undergo subsequent release into the immediate environment and inactivate bacteria. Recent reports illustrate the feasibility and practicality of utilizing GO and GO-hybrids to inactivate a variety of Gram-positive and Gram-negative bacteria. Gurunathan and coworkers[276] applied the nitro blue tetrazolium (NBT) reduction assay to show that both GO and rGO efficiently produce ROS ($O_2^{\bullet-}$) that effectively contribute to the decreased cellular viability of *Pseudomonas aeruginosa*. Kim and coworkers also demonstrated that $O_2^{\bullet-}$ (detected via an XTT assay) generated from a GO-hydride nanocomposite film, GO-MoS_2, could inactivate *E. coli* K-12 (DH5a) cells. In another example illustrating the use of a nanohybrid, Nanda and coworkers[277] prepared a GO-cystamine drug delivery agent and confirmed its effectiveness in mediating the generation of ROS against *E. coli* and three other pathogenic bacteria. GQDs are unique antibacterial materials which share characteristics of both graphene and carbon dots; GQDs

are inherently biocompatible and demonstrate peroxidase-like activity. Sun and coworkers[278] showed that GQDs can, in the presence of low levels of H_2O_2 (1 mmol L^{-1} to 10 mmol L^{-1}), catalyze the formation of $^{\bullet}OH$. The authors demonstrated the effectiveness of the generated $^{\bullet}OH$ to inactivate both *E. coli* and *S. aureus* bacteria, to inhibit biofilm formation and to help heal wounds in mice.

The potential clinical utility of GO antibacterial oxidative coatings for medical devices was recently described by Li and coworkers.[258] In their research, the authors used chemical reduction and hydration procedures to specifically prepare a library of GO materials with known levels of oxidized functional groups and carbon radicals (•C) on their surfaces. The GO library was tested on antibiotic resistant Gram negative (*E. coli*) and Gram-positive (*L. crispatus*) bacteria and the authors noted that the highest bacterial killing was strongly correlated to the GO material with the highest level of hydration (hGO-2) and with the highest level of •C radicals on the surface. The •C radical is formed on GO surfaces during the hydration process as epoxy rings open. The mechanism for the antibacterial effects of the •C radical is based on the presence of unpaired electrons that endow it with a large pro-oxidative potential. The •C radical oxidizes membrane lipids to initiate lipid peroxidation reactions (confirmed by flow cytometry experiments on the bacterial cells) that are lethal to the bacteria. The authors further demonstrated the antibacterial effects of the •C radical by preparing films of hGO-2 on glass substrates and also covalently bonding hGO-2 to the surface of silicone catheters. In both hGO-2 cases, antibiotic resistant *E. coli* suffered increasing levels of membrane damage and fragmentation.

GO and its derivatives have been increasingly investigated as nanocarriers and/or as drug delivery vehicles for the treatment of different types of cancers. GO, because of its flat sp^2-hybridized carbon network can adsorb hydrophobic molecules via π-π stacking and transport these molecules into cells and organs with high efficiencies. In particular, GO has been explored as a carrier for transporting nontoxic dye PSs (the source of the $^1O_2$) into tumors as part of anticancer PDT. The theoretical and experimental utility of GO and its relevant derivatives in PDT has been thoroughly reviewed.[279, 280] Next generation graphene-based PDT agents are based on GQDs[281–283] which have been demonstrated to be biocompatible, to not suffer from photobleaching, and to have extremely large $^1O_2$ quantum yields following visible light irradiation. When utilizing GQDs, the GQD is the actual PDT agent directly producing $^1O_2$; the GQD is not a nanocarrier for a PS. In fact, Ge and coworkers[281] recently synthesized a water dispersible GQD based on the use of a hydrothermal synthetic route that produced the highest $^1O_2$ quantum yield (≈ 1.3) of all currently utilized PDT agents (about twice as high as the best PDT agents). The authors described the successful use of the GQDs in both *in vitro* and *in vivo* exposure scenarios. Following visible light irradiation (405 nm and 633 nm lasers) in the presence of HeLa cells, GQDs induced dose dependent decreases in cellular viability and cell shrinkage. Direct injection of the GQDs into MDA MB-231 tumor-bearing mice in combination with PDT resulted in permanent tumor shrinkage and destruction after 17 d and no tumor regrowth after 50 d in comparison to control mice. It is possible that these emerging PDT agents may also be applicable for combating drug-resistant microorganisms.

The prospects for the further development of graphene-based materials for nanomedicine applications are highly promising, yet concerns regarding the potential long-term toxicity of graphene remain. Current graphene researchers have explicitly expressed the need for methods and data that can be utilized to better characterize the *in vivo* pharmacokinetics and toxicological profiles of graphene materials used for nanomedicinal therapy.[245] The main problem is that graphene-based materials, and specifically GO, are not rapidly eliminated from the body, but instead, are passively retained in the reticuloendothelial system (RES) organs. The kidney is not able to effectively clear NMs larger than about 5 nm,[284] thus GO has to enter the liver and become part of the bile and feces in order to be eliminated. This is a very slow process that can potentially contribute to the long-term toxicity of GO and other graphene-based materials. However, it was recently hypothesized that GO may not be as bio-persistent as expected. Kotchey and coworkers[285, 286] demonstrated that GO, as well as other carbon NMs containing carboxylated functional groups can be rapidly oxidized and degraded over time in the presence of HRP enzyme and H_2O_2. Thus, it is feasible that human-based peroxidases, such as myeloperoxidase, eosinophil peroxidase, and lactoperoxidase may actively contribute to the enzymatic biodegradation of GO and its derivatives *in vivo*. Additional studies on the endogenous biodegradation of GO by human peroxidases is warranted.

Higher Order Carbon Nanomaterials

The initial use of higher-order carbon nanomaterial (CNM) allotropes (fullerenes: Bucky balls, carbon nanotubes (CNTs), carbon quantum dots (CQDs), etc.) in living cellular systems was driven by proposed studies of their basic transport properties and bio-molecular interactions, as well as their cell scaffolding, photonic, membrane sorption, and delivery applications.[287–295] Reports of their unique chemical, structural (size/shape), optical, and electronic (also electrochemical) properties predate their biological use.[296–302] Importantly, the scale of many CNMs is on the same order of magnitude as many biological materials.

The chemical and interfacial properties of carbon fullerenes impart a rich platform for bio-reactive and supramolecular chemistry applications. In regard to their physical properties, carbon fullerenes have large surface areas made of carbon atoms arranged depending on the allotrope in question:[303] CNTs are tube-like hollow fullerenes made of hexagonal lattice repeats of sp^2 hybridized π systems. Their surfaces are graphene-like, rigid, curved, and free of lattice distortions (Figure 1a). The CNTs comprise multi-walled (MWCNT), single-walled (SWCNT), and double-walled (DWCNT) varieties. Diameters range from sub-1 nm to 3 nm for SWCNTs, and can range from 5 nm to 30 nm for MWCNTs. CNTs possess a uniquely large aspect ratio that can surpass a factor of 1000. Stable and individualized CNTs have been prepared at length scales that range from ultra-short 10 nm to μm long. The spherical (Bucky) fullerenes (prototyped by the hexagonal/pentagonal C_{60}) shown in Figure 1b are reported to range in diameter from 0.4 nm to 1.6 nm,[304] and the amorphous-to-crystalline CQDs (discovered during SWCNT purification[305]) depicted in Figure 1c have curved surfaces below 10 nm in diameter.[306–308] Additionally, the single-walled carbon nanohorns (SWCNH, Figure 1d) have interesting cone-like shapes with diameters ≈ 2 to 5 nm that can aggregate into stable star-shaped structures.[309] Lastly, the amorphous carbons (Figure 1e) such as carbon black (e.g. charcoal) and hydrophilic carbon clusters (HCC) are

comprised of distorted carbon lattices that routinely incorporate heteroatom dopants, like oxygen. A notable property of higher-order CNMs is their biological stability—with the possible exception of peroxidase systems in particular immune cells,[310, 311] the lattices of these NMs are resistant to biochemical corrosion.

A common surface property that all CNMs share is hydrophobicity, or a lack of water wettability.[312–314] Hydrophobic effects and van der Waals (Keesom, Debye, and London) forces determine surface and electronic interactions. Therefore, functionality is critical when investigating potential biological redox interactions because, *(1)* CNMs must be functionalized to become soluble for biological use, and *(2)* local environmental and interface properties impact reaction kinetics.[315] Functionalization of CNMs is generally classified into covalent and non-covalent modification.[316] Common non-covalent functionalities include amphiphilic (hydrophobic and hydrophilic) polymers, molecules, and bio-polyelectrolytes such as DNA and carboxymethyl-cellulose. Covalent modifications include direct functionalization of the carbon lattice to attach acids, bases, and other tailored chemistries.

The electrochemistry of higher-order CNMs largely depends on the electronic band structure —metallic, semiconductor, or insulator—of the CNM. The amorphous/glassy nanocarbons,[317, 318] CNTs,[319–323] and Bucky fullerenes[324] have been characterized in detail. In open-circuit aqueous systems such as biological media/serum, the O_2/H_2O redox couple dominates (e.g. see[325–329]) and must be factored into the presence of other interfering redox couples that are not NM targets. Notable interactions and applications of these carbon allotropes are described below.

In semiconducting Bucky fullerenes (Figure 1b), energy input in the form of visible light is a popular means to promote free radical reactions and charge-transfer complexes. $^3O_2$ will interact with excited fullerenes to generate $^1O_2$ or $O_2^{\bullet -}$. This is possible because these fullerenes are stable in various reversible anionic states and have favorable singlet-triplet conversions and lifetimes.[324] Lu et al.[330] employed the fullerene C_{60} in a PDT approach to kill Gram-negative bacteria found in wound infections (*P. aeruginosa and P. mirabilis*), which is a critical issue that can lead to systemic sepsis in emergencies. In contrast, Gram-positive strains tend not to produce sepsis and are readily sensitive to PDT. Previous work found that quaternary pyrrolidinium (cationic) functionalization of C_{60} (BF6) increases the killing of Gram-positive bacteria, Gram-negative bacteria, and fungal yeast.[331] Such fullerenes are thought to act via photo-activated mechanisms that involve $O_2^{\bullet -}$ and $^{\bullet}OH$. *In vitro* culture experiments used a non-coherent lamp with 400 nm to 700 nm white-light band-pass filters to test the visible spectrum. An illumination time of 50 s (10 J/cm^2) was used to show the dose-dependent killing ability of photoactive BF6. For *in vivo* experiments, 2.5×10^7 log-phase bacterial cells were placed onto an excisional wound on the back of BALB/c mice susceptible to terminal septicemia. In the dark, the 15 min BF6-exposed wound produced a minimal reduction, but no trend, in the bioluminescence used to track live *P. mirabilis* bacteria. Survival in these mice was 16 %. White-light illumination of the mice showed a dose-dependent reduction in bioluminescence which translated to a survival of 82 % after 15 d. In contrast, infection of mouse wounds by *P. aeruginosa* behaved differently. BF6 treatment and illumination resulted in a 95 % reduction of bioluminescence;

however, 100 % of mice died from sepsis within 3 d. The authors discovered that the *P. aeruginosa* had recovered after 24 h and had infected surrounding tissue. The authors decided to combine the BF6 with a modest antibiotic regimen (6 mg kg^{-1} Tobramycin for 1 d). The antibiotic alone showed no efficacy, but increased rodent survival to 20 %. When the antibiotic was combined with BF6, the authors found the same dose-dependent reduction in bioluminescence seen with illuminated BF6 alone. However, upon examination after 24 h, there was no bacterial regrowth and no invasion into surrounding tissues. Mouse survival increased to 60 % after 15 d. The authors concluded this study to be the first experimental evidence of a fullerene-mediated curative treatment for a fatal disease in rodents. The authors mention the unusual photochemical mechanism (Type I) was quite effective versus the common Type II mechanism shown in analogous studies. Surprisingly, the authors found that a sub-clinical dose of antibiotic (Tobramycin) therapy could prevent the re-growth of the aggressive strain after BF6 illumination.

Amorphous and glassy carbons (Figure 1e) are generally of metallic or insulating character, depending on their surface features and lattice. The insulating materials are notable for their double-layer capacitive currents and are therefore inert in open-circuit. However, depending on their surface chemistry, reduction-oxidation may occur in highly acidic/alkaline media. A complex oxygen-reduction reaction (ORR), similar to the end product of the mitochondrial respiratory chain, can occur in media pH>7.0.[332] For perspective, this general mechanism underlies iron-mediated cancer cell death induced by another class of insulator-like NPs.[333] Huq et al.[334] utilized bio-compatible PEGylated hydrophilic carbon clusters (HCCs) to scavenge $O_2^{\bullet-}$, and $^{\bullet}OH$. These particles were studied previously for nano-vectors[335] and for their antioxidant action in traumatic brain injury (TBI) models.[336] In rodents, these HCCs accumulate in the spleen, a secondary lymphoid organ, in contrast to canonical NM phagocyte uptake after systemic injection. Maximum blood circulation of HCC was reached 24 h after injection. Versus a carbon black (India ink) control, the authors find their HCCs take a similar lymphatic route but are not internalized by node or thymus macrophages and T lymphocytes. Rather, splenic T-cell uptake selectivity was confirmed *ex vivo*. Interestingly, HCCs are continuously exocytosed/recycled after internalization rather than degraded in the endolysosome. In culture, HCCs reduce intracellular $O_2^{\bullet-}$ levels and therefore the proliferation of antigen-stimulated, myelin protein-specific primary rat $CD4^+$ T-cells. The reduction in intracellular $O_2^{\bullet-}$ requires HCC internalization and effects proliferation indirectly through radical scavenging. Compared to the HCCs, vitamin C and water-soluble vitamin E have no effect on T-cell proliferation. Assay showed that the HCCs exert a selective effect on inflammatory signaling molecules such as IL-2 and INF-γ, but not IL-17A, indicating the anti-oxidant mechanism modulates a distinct signaling pathway. An *in vivo* model of delayed-type hypersensitivity (DHT type IV), which displays memory T-cell-mediated inflammation, was abrogated after a single subcutaneous dose (2 mg/kg) of HCC at the time of immunization or subsequent challenge. A similar result was found after injection of ovalbumin-specific T-cells followed by challenge. The injected T-cells had no homing defect at the inflammation site, indicating the HCCs behave similarly to T-cell immunomodulator drugs on the market. A subsequent test of HCCs in rats with acute autoimmune encephalomyelitis (EAE, a MS model) indicated that subcutaneous HCC treatment every three days after the onset of clinical signs can reduce disease severity

(clinical behavioral score) and inflammatory foci in spinal cord grey matter. Intracellular $O_2^{\bullet-}$ scavenging to modulate T-cell activity, as well as prevent immune cell infiltration into the central nervous system in the EAE model, are interesting and unique applications of these insulator-type carbon clusters.

The CNT properties vary depending on their type (SWCNT, DWCNT, and MWCNT, Figure 1a) since only the limiting (outer) surface is electrochemically active.[337] The metallic (mCNT) or semiconducting (sCNT) band structure dictates reactivity; mCNT are inherently more electroactive in open-circuit when compared to sCNT. The mCNTs are quantum wires that undergo rapid charge accumulation in solution *via* surface functionalization, adsorption, and/or condensation interactions.[325, 338, 339] Compared to Bucky fullerenes, the SWCNT lattice is rather un-stable in an anionic/cationic state (the DW/MWCNT are more stable).[340, 341] This instability suggests that a redox path might be from a biological reductant, NADH, to CNT or CNT-associated functionality (or both), then into water, oxygen, or other relatively oxidizing agents.[342, 343] This should result in no net charge generated on the CNT lattice. The CNT surface functionality (covalent or non-covalent) is thought to be important in this relaxation/transfer process. sCNTs are capacitive materials[319, 320, 344] that seem to promote electronic relaxation of redox species with oxygen in quasi-dark open-circuit conditions.[342, 343, 345, 346] For example, ad-atom cations may mediate this activity.[326, 343] Notwithstanding, a precise path of the transfer is unknown. A similar relaxation mechanism through large bandgap (small diameter) sCNTs may underlie their anti-oxidant protective actions on biopolymers in the presence of dangerous $^{\bullet}OH$ and possibly solvated electrons ($e^{\bullet}$).[347] Otherwise, condensed transition metals like gold ($AuCl_3$) and iridium (K_2IrCl_6) are necessary to transform the sCNT into a canonical electroactive material[339, 348] analogous to platinum electrodes and TiO_2 NPs. Under conditions that favor stable van der Waals interaction with the sCNT, photon energy permits long-lived radical ion pairs with photoactive bioinorganic dyes.[349] sCNT surface delocalized photoexcitations can form ionized carriers whose formation is controlled by extrinsic factors such as excitation fluence, permittivity, surface electrostatics, and chemical environment.[295, 350–358] For these reasons, bio-toxic proteins can be deactivated after high fluence illumination of sCNT produces $O_2^{\bullet-}$ and/or amino acid radicals.[359]

While the photochemical nature of the sCNTs is not fully understood in biological environments, covalent modification of CNTs is used as a means to manipulate ROS generation. For example, based upon prior evidence that *a)* –OH and –COOH functionalized CNTs can chelate metals, *b)* suggestions that CNTs possess antioxidant capability against $^{\bullet}OH$, *c)* some evidence that covalently functionalized CNTs have a greater organic partition coefficient (logP), and *(d)* observations that **π-π** interactions between CNTs and biological electron transport proteins can modulate underlying transport dynamics, Gonzalez-Durruthy et al.[360] tested a battery of CNTs in *ex vivo* mitochondrial preparations for H_2O_2 production (Amplex Red assay) after iron overload. Iron is the most abundant transition metal in the human body and mitochondria can rapidly accumulate Ca^{2+} and Fe^{2+} in pathological situations; the indiscriminate and aggressive nature of $^{\bullet}OH$ radicals produced through Fe^{2+} interaction with H_2O_2 after electron transport chain leak promotes cellular death and disease. The authors tested whether CNTs could modulate this oxidative mechanism. Safranine O was used to confirm the CNTs do not damage mitochondrial

membrane functionality in fractionated preparations. The author's panel of CNTs possessed chemical functionalization-dependent effectiveness against H_2O_2 production by mitochondrial preps from tissues. The authors used cyclic voltammetry (CV) to corroborate the ability of various CNTs to prevent $^{\bullet}OH$ formation from iron-EDTA/H_2O_2 Fenton-Haber-Weiss reactions. Importantly, CV was conducted within an electrochemical potential window corresponding to the potential drop across the mitochondrial redox chain. A fluorometric assay of Fe^{2+} chelation efficiency versus EDTA indicated the mechanism is partially due to the iron-chelating ability of the –COOH functionalized CNTs and possibly the surface π system. CNTs incubated with mitochondrial preps showed no adverse effects on native mitochondrial ion transport systems, further suggesting to the authors that CNTs indirectly impact the ROS producing components of the electron transport chain. In what might be considered a novel melding of application and theory, the authors utilized a QSPR/QSAR chemoinformatics approach to test the prediction that $^{\bullet}OH$ scavenging by CNMs is dependent on functionalization. While this study integrated many disparate concepts, its ability to piece out a possible mechanism through which CNTs synergize with the electron transport chain of the mitochondrion is interesting. It should be noted that a similar concept is thought to operate when non-covalently modified sCNT are delivered into plant chloroplasts for the purpose of augmenting phototransduction.[361]

The quantum-like carbon dots (Figure 1c) show promise given their highly tunable semiconductor bandgap. A favorable bandgap permits visible light excitation and photo-activation for applications in photobiology and phototherapy, reviewed elsewhere.[362, 363] Lastly, recent carbon nanohorn (CNH, Figure 1d) studies highlight the counterintuitive nature of higher-order carbon nanomaterial effects in biology. No distinct changes in intracellular ROS levels or cellular proliferation have been noted after treatment with broad-range concentrations of as-produced or albumin-dispersed CNH,[364, 365] even though these allotropes have semiconductor properties. Interestingly, CNH photosensitization becomes apparent when CNH are pre-oxidized, loaded with photoactive dyes, albumin dispersed, and illuminated.[366] CNHs highlight a key relationship between CNM structure (chemical, electrical, and surface) and function in biological environments.

To conclude, current work on higher-order CNMs in biology has been directed towards several goals: *(1)* the determination of upstream cellular pathways that detect/diagnose the presence and/or reactivity of CNMs. This remains an active area of nanotoxicology. *(2)* The standardization and evaluation of material preparation procedures to address material artifacts and reproducibility.[367, 368] *(3)* Particular challenges related to bio-redox assay cross-interactions with the NM itself.[369] *(4)* Research that seeks to impart selectivity and in some cases specificity to NM reactivity in biological systems through functionalization and surface science. The applications reviewed above highlight the potential promise of CNMs in redox targeted medicine and in basic studies of bio-nano interactions.

Future Perspectives

Within the framework of the previously described nanomedicine modalities, a common thread which connects them all together is the ongoing concern related to their potential adverse effects on human health and safety. The understanding, characterization and

evaluation of the potential acute and/or chronic toxicological properties of NMs is as important to nanomedicine applications in the healthcare industry, as it is for the consumer products, agriculture and electronics industries.[370–372] While it is certainly true that no commercial non-nano based medicine is absolutely free of toxicity or potential adverse effects,[373] it is practical and worthwhile from both a safety and ethical point-of-view to try to design out toxicity in nanomedicines or to develop safer-by-design nanomedicines where functionality is optimized and toxicity is minimized. In cases where the nanomedicine functionality is based on redox-activity, completely designing out biological reactivity may be illogical, but what would be logical is to have a more complete understanding of how the base NM induces off-target effects on the immune system, nervous system, macrophages, etc. To achieve this outcome, we will need to move away from a focus on descriptive toxicology to an emphasis on predictive toxicology. There are simply too many different types and formulations of NMs, such that it is not practical to evaluate on a case-by-case basis an exponentially growing number of NMs utilized in the potential formulation of nanomedicines or medical materials. Alternative testing strategies that use predictive toxicology models and high content screening of cellular models to predict NM toxicity to humans may be a viable option, which warrants serious consideration.[374–377]

Supplementary Material

Refer to Web version on PubMed Central for supplementary material.

Acknowledgments

C.M.S. acknowledges funding and support from the National Academy of Sciences - National Research Council Postdoctoral Research Associateship Program. D.A.H. recognizes support from the NIH New Innovator Award (DP2-HD075698), the Cancer Center Support Grant and Center for Molecular Imaging and Nanotechnology at Memorial Sloan Kettering Cancer Center (P30 CA008748), Honorable Tina Brozman Foundation for Ovarian Cancer Research, Frank A. Howard Scholars Program, Cycle for Survival, Alan and Sandra Gerry Metastasis Research Initiative, Mr. William H. Goodwin and Mrs. Alice Goodwin and the Commonwealth Foundation for Cancer Research, The Experimental Therapeutics Center of MSKCC, and the Imaging & Radiation Sciences Program at MSKCC. C.P.H. is supported by an NIH NCI T-32 graduate training fellowship (CA062948-22) from the Weill Graduate School. The authors would also like to thank P.V. Jena of the Memorial Sloan Kettering Cancer Center for editorial assistance. K.R.R. acknowledges funding and support from Swarthmore College and the Consortium for Faculty Diversity in Liberal Arts Colleges. DNA (PDB 3BSE) and protein (PDB 2F6L) images used in the table of contents graphic were generated by Amanda S. Altieri of the University of Maryland Institute for Bioscience and Biotechnology Research (IBBR).

List of Abbreviated Terms

Ag-CS NC	AgNP-chitosan nanocarriers
AgNPs	silver nanoparticles
AML	acute myeloid leukemia
ALZ	Alzheimer’s disease
AuNCs	gold nanoclusters
AuNPs	gold nanoparticles

BF6	quaternary pyrrolidinium (cationic) functionalization of C_{60}
β-lap	β-lapachone
CMP	cell membrane potential
CNMs	carbon nanomaterials
CNPs	cerium oxide nanoparticles
CNTs	carbon nanotubes
COOH-GO	carboxylated graphene oxide
CQDs	carbon quantum dots
CV	cyclic voltammetry
DHT type IV	delayed-type hypersensitivity
DNA	deoxyribonucleic acid
DWCNTs	double-walled carbon nanotubes
EAE	acute autoimmune encephalomyelitis
EDTA	ethylenediaminetetraacetic acid
EGCG	epigallocatechin-3-gallate
ESR	electron spin resonance
Fe_3O_4	magnetite
γ-Fe_2O_3	maghemite
FLG	few-layer-graphene
G	graphene
GO	graphene oxide
rGO	reduced graphene oxide
GQDs	graphene quantum dots
GSH	glutathione
GSSG	glutathione disulfide
H_2O_2	hydrogen peroxide
HCCs	hydrophilic carbon clusters
HNE	4-hydroxy-2-nonenal

HP	*Hamelia patens* leaf extract
HRP	horseradish peroxidase
IONs	iron oxide nanoparticles
JNK	c-Jun N-terminal kinase
MIRB	Molday ION Rhodamine B
MMP	mitochondrial membrane potential
MRI	magnetic resonance imaging
MS	multiple sclerosis
MWCNTs	multi-walled carbon nanotubes
NAC	N-acetyl cysteine
NIR	near-infrared
NMs	nanomaterials
NPs	nanoparticles
NSCs	neural stem cells
$^{\bullet}$OH	hydroxyl radical
$^{\bullet}$OOH	hydroperoxyl radical
$O_2^{\bullet-}$	superoxide anion radical
ORR	oxygen-reduction reaction
PARP1	poly(ADP-ribose) polymerase 1
PDT	photodynamic therapy
PEG	polyethylene glycol
PEG-b-PDPA	poly(ethyleneglycol)-b-polu(2-(2-diisopropylamino) ethyl methacrylate
PpIX	protoporphyrin IX
PSs	photosensitizers
PS*	singlet excited state photosensitizers
PS**	triplet excited state photosensitizers
PTX	paclitaxel
PVP	polyvinylpyrrolidone

ROS	reactive oxygen species
sCNTs	semiconducting carbon nanotubes
SeNP	selenium nanoparticles
SMA	smooth muscle actin
SOD	superoxide dismutase
SPIONs	superparamagnetic iron oxide nanoparticles
SWCNHs	single-walled carbon nanohorns
SWCNTs	single-walled carbon nanotubes
TiO_2NMs	titanium dioxide nanomaterials
TiO_2NPs	titanium dioxide nanoparticles
TMB	3,3,5,5-tetramethylbenzidine
UV	ultraviolet

References

1. Caruso F, Hyeon T, Rotello VM. Chemical Society Reviews. 2012; 41:2537–2538. [PubMed: 22388450]
2. Doane TL, Burda C. Chemical Society Reviews. 2012; 41:2885–2911. [PubMed: 22286540]
3. Min Y, Caster JM, Eblan MJ, Wang AZ. Chemical Reviews. 2015; 115:11147–11190. [PubMed: 26088284]
4. Pelaz B, Alexiou C, Alvarez-Puebla RA, Alves F, Andrews AM, Ashraf S, Balogh LP, Ballerini L, Bestetti A, Brendel C, Bosi S, Carril M, Chan WCW, Chen C, Chen X, Chen X, Cheng Z, Cui D, Du J, Dullin C, Escudero A, Feliu N, Gao M, George M, Gogotsi Y, Grünweller A, Gu Z, Halas NJ, Hampp N, Hartmann RK, Hersam MC, Hunziker P, Jian J, Jiang X, Jungebluth P, Kadhiresan P, Kataoka K, Khademhosseini A, Kopeček J, Kotov NA, Krug HF, Lee DS, Lehr C-M, Leong KW, Liang X-J, Ling Lim M, Liz-Marzán LM, Ma X, Macchiarini P, Meng H, Möhwald H, Mulvaney P, Nel AE, Nie S, Nordlander P, Okano T, Oliveira J, Park TH, Penner RM, Prato M, Puntes V, Rotello VM, Samarakoon A, Schaak RE, Shen Y, Sjöqvist S, Skirtach AG, Soliman MG, Stevens MM, Sung H-W, Tang BZ, Tietze R, Udugama BN, VanEpps JS, Weil T, Weiss PS, Willner I, Wu Y, Yang L, Yue Z, Zhang Q, Zhang Q, Zhang X-E, Zhao Y, Zhou X, Parak WJ. ACS Nano. 2017; doi: 10.1021/acsnano.6b06040
5. Karakoti A, Singh S, Dowding JM, Seal S, Self WT. Chem Soc Rev. 2010; 39:4422–4432. [PubMed: 20717560]
6. Rzigalinski BA, Meehan K, Davis RM, Xu Y, Miles WC, Cohen CA. Nanomedicine. 2006; 1:399–412. [PubMed: 17716143]
7. Birben E, Sahiner UM, Sackesen C, Erzurum S, Kalayci O. The World Allergy Organization journal. 2012; 5:9–19. [PubMed: 23268465]
8. Uttara B, Singh AV, Zamboni P, Mahajan RT. Current Neuropharmacology. 2009; 7:65–74. [PubMed: 19721819]
9. Pham-Huy LA, He H, Pham-Huy C. International Journal of Biomedical Science : IJBS. 2008; 4:89–96. [PubMed: 23675073]
10. Waris G, Ahsan H. Journal of Carcinogenesis. 2006; 5:14–14. [PubMed: 16689993]
11. Winterbourn CC. Free Radical Biology and Medicine. 2015; 80:164–170. [PubMed: 25277419]

12. Valko M, Rhodes CJ, Moncol J, Izakovic M, Mazur M. Chemico-Biological Interactions. 2006; 160:1–40. [PubMed: 16430879]
13. Markesbery WR. Free Radical Biology and Medicine. 1997; 23:134–147. [PubMed: 9165306]
14. Ide T, Tsutsui H, Hayashidani S, Kang D, Suematsu N, Nakamura K-i, Utsumi H, Hamasaki N, Takeshita A. Circulation Research. 2001; 88:529. [PubMed: 11249877]
15. Hybertson BM, Gao B, Bose SK, McCord JM. Molecular Aspects of Medicine. 2011; 32:234–246. [PubMed: 22020111]
16. Korsvik C, Patil S, Seal S, Self WT. Chem Commun (Camb). 2007; :1056–1058.doi: 10.1039/b615134e [PubMed: 17325804]
17. Pirmohamed T, Dowding JM, Singh S, Wasserman B, Heckert E, Karakoti AS, King JES, Seal S, Self WT. Chemical Communications. 2010; 46:2736–2738. [PubMed: 20369166]
18. Li N, Xia T, Nel AE. Free Radic Biol Med. 2008; 44:1689–1699. [PubMed: 18313407]
19. Yang H, Liu C, Yang D, Zhang H, Xi Z. Journal of Applied Toxicology. 2009; 29:69–78. [PubMed: 18756589]
20. Dolmans DEJGJ, Fukumura D, Jain RK. Nat Rev Cancer. 2003; 3:380–387. [PubMed: 12724736]
21. Henderson BW, Dougherty TJ. Photochemistry and Photobiology. 1992; 55:145–157. [PubMed: 1603846]
22. Laurent S, Forge D, Port M, Roch A, Robic C, Vander Elst L, Muller RN. Chemical Reviews. 2008; 108:2064–2110. [PubMed: 18543879]
23. Meng Lin M, Kim H-H, Kim H, Muhammed M, Kyung Kim D. Nano Reviews. 2010; 1:4883.
24. Mahmoudi M, Sant S, Wang B, Laurent S, Sen T. Advanced Drug Delivery Reviews. 2011; 63:24–46. [PubMed: 20685224]
25. Wahajuddin, Arora S. Int J Nanomedicine. 2012; 7:3445–3471. [PubMed: 22848170]
26. Singh N, Jenkins GJS, Asadi R, Doak SH. Nano Reviews. 2010; 1:5358.
27. Guardia P, Di Corato R, Lartigue L, Wilhelm C, Espinosa A, Garcia-Hernandez M, Gazeau F, Manna L, Pellegrino T. ACS Nano. 2012; 6:3080–3091. [PubMed: 22494015]
28. Muthiah M, Park I-K, Cho C-S. Biotechnology Advances. 2013; 31:1224–1236. [PubMed: 23528431]
29. Ling D, Hyeon T. Small. 2013; 9:1450–1466. [PubMed: 23233377]
30. Liu G, Gao J, Ai H, Chen X. Small. 2013; 9:1533–1545. [PubMed: 23019129]
31. Lee N, Yoo D, Ling D, Cho MH, Hyeon T, Cheon J. Chemical Reviews. 2015; 115:10637–10689. [PubMed: 26250431]
32. Mahmoudi M, Laurent S, Shokrgozar MA, Hosseinkhani M. ACS Nano. 2011; 5:7263–7276. [PubMed: 21838310]
33. Tartaj P, Morales MP, Gonzalez-Carreño T, Veintemillas-Verdaguer S, Serna CJ. Advanced Materials. 2011; 23:5243–5249. [PubMed: 22299136]
34. Winterbourn CC. Toxicology Letters. 1995; 82:969–974. [PubMed: 8597169]
35. Kehrer JP. Toxicology. 2000; 149:43–50. [PubMed: 10963860]
36. Singh N, Jenkins GJ, Nelson BC, Marquis BJ, Maffeis TG, Brown AP, Williams PM, Wright CJ, Doak SH. Biomaterials. 2012; 33:163–170. [PubMed: 22027595]
37. Luo C, Li Y, Yang L, Wang X, Long J, Liu J. Archives of Toxicology. 2015; 89:357–369. [PubMed: 24847785]
38. Lunov O, Syrovets T, Büchele B, Jiang X, Röcker C, Tron K, Nienhaus GU, Walther P, Mailänder V, Landfester K, Simmet T. Biomaterials. 2010; 31:5063–5071. [PubMed: 20381862]
39. Vogel CFA, Charrier JG, Wu D, McFall AS, Li W, Abid A, Kennedy IM, Anastasio C. Free Radical Research. 2016; 50:1153–1164. [PubMed: 27558512]
40. Al Faraj A, Shaik AP, Shaik AS. Nanotoxicology. 2015; 9:825–834. [PubMed: 26356541]
41. Sabareeswaran A, Ansar EB, Harikrishna Varma PRV, Mohanan PV, Kumary TV. Nanomedicine: Nanotechnology, Biology and Medicine. 2016; 12:1523–1533.
42. Hauser AK, Mitov MI, Daley EF, McGarry RC, Anderson KW, Hilt JZ. Biomaterials. 2016; 105:127–135. [PubMed: 27521615]

43. Gao L, Zhuang J, Nie L, Zhang J, Zhang Y, Gu N, Wang T, Feng J, Yang D, Perrett S, Yan X. Nat Nano. 2007; 2:577–583.
44. Fan J, Yin J-J, Ning B, Wu X, Hu Y, Ferrari M, Anderson GJ, Wei J, Zhao Y, Nie G. Biomaterials. 2011; 32:1611–1618. [PubMed: 21112084]
45. Chen Z, Yin J-J, Zhou Y-T, Zhang Y, Song L, Song M, Hu S, Gu N. ACS Nano. 2012; 6:4001–4012. [PubMed: 22533614]
46. Huang G, Chen H, Dong Y, Luo X, Yu H, Moore Z, Bey EA, Boothman DA, Gao J. Theranostics. 2013; 3:116–126. [PubMed: 23423156]
47. Pongrac IM, Pavičić I, Milić M, Brkić Ahmed L, Babič M, Horák D, Vinković Vrček I, Gajović S. International Journal of Nanomedicine. 2016; 11:1701–1715. [PubMed: 27217748]
48. Gimble JM, Katz AJ, Bunnell BA. Circulation Research. 2007; 100:1249. [PubMed: 17495232]
49. Hoehn M, Wiedermann D, Justicia C, Ramos-Cabrer P, Kruttwig K, Farr T, Himmelreich U. The Journal of Physiology. 2007; 584:25–30. [PubMed: 17690140]
50. Umashankar A, Corenblum MJ, Ray S, Valdez M, Yoshimaru ES, Trouard TP, Madhavan L. International Journal of Nanomedicine. 2016; 11:1731–1748. [PubMed: 27175074]
51. Wu M, Gu L, Gong Q, Sun J, Ma Y, Wu H, Wang Y, Guo G, Li X, Zhu H. Nanomedicine. 2017; 12:555–570. [PubMed: 28181458]
52. Reed K, Cormack A, Kulkarni A, Mayton M, Sayle D, Klaessig F, Stadler B. Environmental Science: Nano. 2014; 1:390–405.
53. Tarnuzzer RW, Colon J, Patil S, Seal S. Nano Letters. 2005; 5:2573–2577. [PubMed: 16351218]
54. Chen J, Patil S, Seal S, McGinnis JF. Nat Nano. 2006; 1:142–150.
55. Schubert D, Dargusch R, Raitano J, Chan S-W. Biochemical and Biophysical Research Communications. 2006; 342:86–91. [PubMed: 16480682]
56. Celardo I, Pedersen JZ, Traversa E, Ghibelli L. Nanoscale. 2011; 3:1411–1420. [PubMed: 21369578]
57. Das S, Dowding JM, Klump KE, McGinnis JF, Self W, Seal S. Nanomedicine. 2013; 8:1483–1508. [PubMed: 23987111]
58. Walkey C, Das S, Seal S, Erlichman J, Heckman K, Ghibelli L, Traversa E, McGinnis JF, Self WT. Environmental Science: Nano. 2015; 2:33–53. [PubMed: 26207185]
59. Esch F, Fabris S, Zhou L, Montini T, Africh C, Fornasiero P, Comelli G, Rosei R. Science. 2005; 309:752–755. [PubMed: 16051791]
60. Kuchma MH, Komanski CB, Colon J, Teblum A, Masunov AE, Alvarado B, Babu S, Seal S, Summy J, Baker CH. Nanomedicine: Nanotechnology, Biology and Medicine. 2010; 6:738–744.
61. Tan F, Zhang Y, Wang J, Wei J, Cai Y, Qian X. Journal of Mass Spectrometry. 2008; 43:628–632. [PubMed: 18076124]
62. Asati A, Kaittanis C, Santra S, Perez JM. Analytical Chemistry. 2011; 83:2547–2553. [PubMed: 21370817]
63. Asati A, Santra S, Kaittanis C, Nath S, Perez JM. Angewandte Chemie International Edition. 2009; 48:2308–2312. [PubMed: 19130532]
64. Jiao X, Song H, Zhao H, Bai W, Zhang L, Lv Y. Analytical Methods. 2012; 4:3261–3267.
65. Dowding JM, Das S, Kumar A, Dosani T, McCormack R, Gupta A, Sayle TXT, Sayle DC, von Kalm L, Seal S, Self WT. ACS Nano. 2013; 7:4855–4868. [PubMed: 23668322]
66. Andreescu D, Bulbul G, Ozel RE, Hayat A, Sardesai N, Andreescu S. Environmental Science: Nano. 2014; 1:445–458.
67. Nelson BC, Johnson ME, Walker ML, Riley KR, Sims CM. Antioxidants (Basel). 2016; 5:15.
68. Charbgoo F, Ahmad MB, Darroudi M. International Journal of Nanomedicine. 2017; 12:1401–1413. [PubMed: 28260887]
69. Bartley MG, Marquardt K, Kirchhof D, Wilkins HM, Patterson D, Linseman DA. J Alzheimers Dis. 2012; 28:855–868. [PubMed: 22133762]
70. Kwon HJ, Cha M-Y, Kim D, Kim DK, Soh M, Shin K, Hyeon T, Mook-Jung I. ACS Nano. 2016; 10:2860–2870. [PubMed: 26844592]

71. Heckman KL, DeCoteau W, Estevez A, Reed KJ, Costanzo W, Sanford D, Leiter JC, Clauss J, Knapp K, Gomez C, Mullen P, Rathbun E, Prime K, Marini J, Patchefsky J, Patchefsky AS, Hailstone RK, Erlichman JS. ACS Nano. 2013; 7:10582–10596. [PubMed: 24266731]
72. Davan R, Prasad R, Jakka VS, Aparna R, Phani A, Jacob B, Salins PC, Raju D. Journal of Bionanoscience. 2012; 6:78–83.
73. Chigurupati S, Mughal MR, Okun E, Das S, Kumar A, McCaffery M, Seal S, Mattson MP. Biomaterials. 2013; 34:2194–2201. [PubMed: 23266256]
74. Jackson AL, Loeb LA. Mutation Research/Fundamental and Molecular Mechanisms of Mutagenesis. 2001; 477:7–21. [PubMed: 11376682]
75. Storz P. Front Biosci. 2005; 10:1881–1896. [PubMed: 15769673]
76. Alili L, Sack M, von Montfort C, Giri S, Das S, Carroll KS, Zanger K, Seal S, Brenneisen P. Antioxidants & Redox Signaling. 2013; 19:765–778. [PubMed: 23198807]
77. von Montfort C, Alili L, Teuber-Hanselmann S, Das S, Seal S, Brenneisen P. Redox Biology. 2015; 5:424. [PubMed: 28162295]
78. Yokel RA, Hussain S, Garantziotis S, Demokritou P, Castranova V, Cassee FR. Environmental Science: Nano. 2014; 1:406–428. [PubMed: 25243070]
79. Yokel RA, Florence RL, Unrine JM, Tseng MT, Graham UM, Wu P, Grulke EA, Sultana R, Hardas SS, Butterfield DA. Nanotoxicology. 2009; 3:234–248.
80. Hirst SM, Karakoti A, Singh S, Self W, Tyler R, Seal S, Reilly CM. Environ Toxicol. 2013; 28:107–118. [PubMed: 21618676]
81. Aw MS, Simovic S, Addai-Mensah J, Losic D. Journal of Materials Chemistry. 2011; 21:7082–7089.
82. Jarosz M, Pawlik A, Szuwarzyński M, Jaskuła M, Sulka GD. Colloids and Surfaces B: Biointerfaces. 2016; 143:447–454. [PubMed: 27037782]
83. Gultepe E, Nagesha D, Casse BDF, Banyal R, Fitchorov T, Karma A, Amiji M, Sridhar S. Small. 2010; 6:213–216. [PubMed: 19967712]
84. Kunze J, Müller L, Macak JM, Greil P, Schmuki P, Müller FA. Electrochimica Acta. 2008; 53:6995–7003.
85. Sun J, Petersen EJ, Watson SS, Sims CM, Kassman A, Frukhtbeyn S, Skrtic D, Ok MT, Jacobs DS, Reipa V, Ye Q, Nelson BC. Acta Biomater. 2017; doi: 10.1016/j.actbio.2017.01.084
86. Azhang H, Suman S-R, Christos T, Mathew TM, Cortino S, Alexander LY, Tolou S. Journal of Physics D: Applied Physics. 2015; 48:275401.
87. Rehman FU, Zhao C, Jiang H, Wang X. Biomaterials Science. 2016; 4:40–54. [PubMed: 26442645]
88. Zhang S, Yang D, Jing D, Liu H, Liu L, Jia Y, Gao M, Guo L, Huo Z. Nano Research. 2014; 7:1659–1669.
89. Cai R, Kubota Y, Shuin T, Sakai H, Hashimoto K, Fujishima A. Cancer Research. 1992; 52:2346–2348. [PubMed: 1559237]
90. Wang Y, Cui H, Zhou J, Li F, Wang J, Chen M, Liu Q. Environmental Science and Pollution Research. 2015; 22:5519–5530. [PubMed: 25339530]
91. Huang, N-p, Min-hua, X., Yuan, C-w, Rui-rong, Y. Journal of Photochemistry and Photobiology A: Chemistry. 1997; 108:229–233.
92. Lagopati N, Tsilibary EP, Falaras P, Papazafiri P, Pavlatou EA, Kotsopoulou E, Kitsiou P. Int J Nanomedicine. 2014; 9:3219–3230. [PubMed: 25061298]
93. Manke A, Wang L, Rojanasakul Y. BioMed Research International. 2013; 2013:15.
94. Ramkumar KM, Manjula C, GnanaKumar G, Kanjwal MA, Sekar TV, Paulmurugan R, Rajaguru P. European Journal of Pharmaceutics and Biopharmaceutics. 2012; 81:324–333. [PubMed: 22446064]
95. Bernardeschi M, Guidi P, Scarcelli V, Frenzilli G, Nigro M. Anal Bioanal Chem. 2010; 396:619–623. [PubMed: 19915826]
96. Ghosh M, Bandyopadhyay M, Mukherjee A. Chemosphere. 2010; 81:1253–1262. [PubMed: 20884039]

97. Kang SJ, Kim BM, Lee YJ, Chung HW. Environmental and molecular mutagenesis. 2008; 49:399–405. [PubMed: 18418868]

98. Turkez H. Experimental and toxicologic pathology : official journal of the Gesellschaft fur Toxikologische Pathologie. 2011; 63:453–457. [PubMed: 20346638]

99. Aw MS, Addai-Mensah J, Losic D. Chemical Communications. 2012; 48:3348–3350. [PubMed: 22367413]

100. Moosavi MA, Rahmati M. Austin Therapeutics. 2015; 2:1–2.

101. Yadav HM, Thorat ND, Yallapu MM, Tofail SAM, Kim J-S. Journal of Materials Chemistry B. 2017; 5:1461–1470.

102. Chen HW, Su SF, Chien CT, Lin WH, Yu SL, Chou CC, Chen JJ, Yang PC. FASEB journal : official publication of the Federation of American Societies for Experimental Biology. 2006; 20:2393–2395. [PubMed: 17023518]

103. Gurr JR, Wang AS, Chen CH, Jan KY. Toxicology. 2005; 213:66–73. [PubMed: 15970370]

104. Hussain SM, Hess KL, Gearhart JM, Geiss KT, Schlager JJ. Toxicol In Vitro. 2005; 19:975–983. [PubMed: 16125895]

105. Sayes CM, Wahi R, Kurian PA, Liu Y, West JL, Ausman KD, Warheit DB, Colvin VL. Toxicol Sci. 2006; 92:174–185. [PubMed: 16613837]

106. Thevenot P, Cho J, Wavhal D, Timmons RB, Tang L. Nanomedicine. 2008; 4:226–236. [PubMed: 18502186]

107. Zhu Y, Eaton JW, Li C. PLoS One. 2012; 7:e50607. [PubMed: 23185639]

108. Myroshnychenko V, Rodriguez-Fernandez J, Pastoriza-Santos I, Funston AM, Novo C, Mulvaney P, Liz-Marzan LM, Garcia de Abajo FJ. Chem Soc Rev. 2008; 37:1792–1805. [PubMed: 18762829]

109. Cobley CM, Chen J, Cho EC, Wang LV, Xia Y. Chem Soc Rev. 2011; 40:44–56. [PubMed: 20818451]

110. Webb JA, Bardhan R. Nanoscale. 2014; 6:2502–2530. [PubMed: 24445488]

111. Ashraf, S., Pelaz, B., del Pino, P., Carril, M., Escudero, A., Parak, WJ., Soliman, MG., Zhang, Q., Carrillo-Carrion, C. Light-Responsive Nanostructured Systems for Applications in Nanomedicine. Sortino, S., editor. Springer International Publishing; Cham: 2016. p. 169-202.

112. Holzinger M, Le Goff A, Cosnier S. Front Chem. 2014; 2:63. [PubMed: 25221775]

113. Sasidharan A, Monteiro-Riviere NA. Wiley Interdiscip Rev Nanomed Nanobiotechnol. 2015; 7:779–796. [PubMed: 25808787]

114. Bhattacharyya S, Kudgus RA, Bhattacharya R, Mukherjee P. Pharm Res. 2011; 28:237–259. [PubMed: 21104301]

115. Arvizo R, Bhattacharya R, Mukherjee P. Expert Opin Drug Deliv. 2010; 7:753–763. [PubMed: 20408736]

116. Willner I, Baron R, Willner B. Biosens Bioelectron. 2007; 22:1841–1852. [PubMed: 17071070]

117. Pingarrón JM, Yáñez-Sedeño P, González-Cortés A. Electrochimica Acta. 2008; 53:5848–5866.

118. Andreescu S, Luck LA. Anal Biochem. 2008; 375:282–290. [PubMed: 18211816]

119. Zhang Y, Wei Q. Journal of Electroanalytical Chemistry. 2016; 781:401–409.

120. Guo S, Wang E. Anal Chim Acta. 2007; 598:181–192. [PubMed: 17719891]

121. Guo S, Dong S. TrAC Trends in Analytical Chemistry. 2009; 28:96–109.

122. Huo X, Liu X, Liu J, Sukumaran P, Alwarappan S, Wong DKY. Electroanalysis. 2016; 28:1730–1749.

123. Wang J. Microchimica Acta. 2012; 177:245–270.

124. Saxena U, Das AB. Biosens Bioelectron. 2016; 75:196–205. [PubMed: 26319162]

125. Teh Y, Jambek AB, Hashim U. Sensor Review. 2016; 36:303–311.

126. Ciganda R, Li N, Deraedt C, Gatard S, Zhao P, Salmon L, Hernandez R, Ruiz J, Astruc D. Chem Commun (Camb). 2014; 50:10126–10129. [PubMed: 25051189]

127. Siddiqi NJ, Abdelhalim MAK, El-Ansary AK, Alhomida AS, Ong WY. Journal of Neuroinflammation. 2012; 9:123. [PubMed: 22691312]

128. Li JJ, Zou L, Hartono D, Ong CN, Bay BH, Lanry Yung LY. Advanced Materials. 2008; 20:138–142.
129. Vecchio G, Galeone A, Brunetti V, Maiorano G, Sabella S, Cingolani R, Pompa PP. PLoS One. 2012; 7:e29980. [PubMed: 22238688]
130. Tedesco S, Doyle H, Redmond G, Sheehan D. Mar Environ Res. 2008; 66:131–133. [PubMed: 18378295]
131. Volland M, Hampel M, Martos-Sitcha JA, Trombini C, Martínez-Rodríguez G, Blasco J. Environmental Science and Pollution Research. 2015; 22:17414–17424. [PubMed: 25994271]
132. Wang P, Wang X, Wang L, Hou X, Liu W, Chen C. Sci Technol Adv Mater. 2015; 16:034610. [PubMed: 27877797]
133. Nethi SK, Mukherjee S, Veeriah V, Barui AK, Chatterjee S, Patra CR. Chemical Communications. 2014; 50:14367–14370. [PubMed: 25298204]
134. Khaing Oo MK, Yang Y, Hu Y, Gomez M, Du H, Wang H. ACS Nano. 2012; 6:1939–1947. [PubMed: 22385214]
135. Di Bucchianico S, Fabbrizi MR, Cirillo S, Uboldi C, Gilliland D, Valsami-Jones E, Migliore L. International Journal of Nanomedicine. 2014; 9:2191–2204. [PubMed: 24855356]
136. Cademartiri L, Kitaev V. Nanoscale. 2011; 3:3435–3446. [PubMed: 21796281]
137. Jin R. Nanoscale. 2010; 2:343–362. [PubMed: 20644816]
138. Wang H-H, Su C-H, Wu Y-J, Lin C-AJ, Lee C-H, Shen J-L, Chan W-H, Chang WH, Yeh H-I. International Journal of Gerontology. 2012; 6:1–4.
139. Lu Y, Chen W. Chem Soc Rev. 2012; 41:3594–3623. [PubMed: 22441327]
140. Cui M, Zhao Y, Song Q. TrAC Trends in Analytical Chemistry. 2014; 57:73–82.
141. Koh TW, Hiszpanski AM, Sezen M, Naim A, Galfsky T, Trivedi A, Loo YL, Menon V, Rand BP. Nanoscale. 2015; 7:9140–9146. [PubMed: 25926355]
142. Luo Z, Zheng K, Xie J. Chem Commun (Camb). 2014; 50:5143–5155. [PubMed: 24266029]
143. Zarschler K, Rocks L, Licciardello N, Boselli L, Polo E, Garcia KP, De Cola L, Stephan H, Dawson KA. Nanomedicine. 2016; 12:1663–1701. [PubMed: 27013135]
144. Tao Y, Li M, Ren J, Qu X. Chem Soc Rev. 2015; 44:8636–8663. [PubMed: 26400655]
145. Zhang L, Wang E. Nano Today. 2014; 9:132–157.
146. Nie L, Xiao X, Yang H. Journal of Nanoscience and Nanotechnology. 2016; 16:8164–8175.
147. Quinn BM, Liljeroth P, Ruiz V, Laaksonen T, Kontturi K. Journal of the American Chemical Society. 2003; 125:6644–6645. [PubMed: 12769569]
148. Antonello S, Holm AH, Instuli E, Maran F. Journal of the American Chemical Society. 2007; 129:9836–9837. [PubMed: 17658798]
149. Schmid G, Simon U. Chem Commun (Camb). 2005; :697–710.doi: 10.1039/b411696h [PubMed: 15685311]
150. Subramaniam C, Pradeep T, Chakrabarti J. Phys Rev Lett. 2005; 95:164501. [PubMed: 16241803]
151. Murray RW. Chemical Reviews. 2008; 108:2688–2720. [PubMed: 18558753]
152. Lee D, Donkers RL, Wang G, Harper AS, Murray RW. Journal of the American Chemical Society. 2004; 126:6193–6199. [PubMed: 15137785]
153. Lopez-Acevedo O, Kacprzak KA, Akola J, Hakkinen H. Nat Chem. 2010; 2:329–334. [PubMed: 21124516]
154. Zhu M, Eckenhoff WT, Pintauer T, Jin R. The Journal of Physical Chemistry C. 2008; 112:14221–14224.
155. Kumar SS, Kwak K, Lee D. Anal Chem. 2011; 83:3244–3247. [PubMed: 21456614]
156. Kwak K, Kumar SS, Pyo K, Lee D. ACS Nano. 2014; 8:671–679. [PubMed: 24350837]
157. Santhosh M, Chinnadayyala SR, Singh NK, Goswami P. Bioelectrochemistry. 2016; 111:7–14. [PubMed: 27126550]
158. Priya C, Sivasankari G, Narayanan SS. Colloids Surf B Biointerfaces. 2012; 97:90–96. [PubMed: 22609587]

159. Shiang YC, Huang CC, Chang HT. Chem Commun (Camb). 2009; :3437–3439.doi: 10.1039/b901916b [PubMed: 19503896]
160. Jiang Y, Wang M, Hardie J, Tonga GY, Ray M, Xu Q, Rotello VM. Small. 2016; 12:3775–3779. [PubMed: 27295172]
161. Lei Q, Hu JJ, Rong L, Cheng H, Sun YX, Zhang XZ. Molecules. 2016:21.
162. Nel A, Xia T, Madler L, Li N. Science. 2006; 311:622–627. [PubMed: 16456071]
163. Khlebtsov N, Dykman L. Chem Soc Rev. 2011; 40:1647–1671. [PubMed: 21082078]
164. Catalan-Figueroa J, Palma-Florez S, Alvarez G, Fritz HF, Jara MO, Morales JO. Nanomedicine. 2015; 11:171–187. [PubMed: 26653284]
165. Xu H, Qu F, Xu H, Lai W, Andrew Wang Y, Aguilar ZP, Wei H. Biometals. 2012; 25:45–53. [PubMed: 21805351]
166. Quinteros MA, Cano Aristizábal V, Dalmasso PR, Paraje MG, Páez PL. Toxicology in Vitro. 2016; 36:216–223. [PubMed: 27530963]
167. Siritongsuk P, Hongsing N, Thammawithan S, Daduang S, Klaynongsruang S, Tuanyok A, Patramanon R. PLoS One. 2016; 11:e0168098. [PubMed: 27977746]
168. Dasgupta N, Ramalingam C. Environmental Chemistry Letters. 2016; 14:477–485.
169. Seong M, Lee DG. Curr Microbiol. 2017; doi: 10.1007/s00284-017-1235-9
170. Jain J, Arora S, Rajwade JM, Omray P, Khandelwal S, Paknikar KM. Molecular Pharmaceutics. 2009; 6:1388–1401. [PubMed: 19473014]
171. Slane J, Vivanco J, Rose W, Ploeg H-L, Squire M. Materials Science and Engineering: C. 2015; 48:188–196. [PubMed: 25579913]
172. Pollini M, Paladini F, Catalano M, Taurino A, Licciulli A, Maffezzoli A, Sannino A. J Mater Sci Mater Med. 2011; 22:2005–2012. [PubMed: 21691829]
173. Kokura S, Handa O, Takagi T, Ishikawa T, Naito Y, Yoshikawa T. Nanomedicine: Nanotechnology, Biology and Medicine. 2010; 6:570–574.
174. Jung JH, Hwang GB, Lee JE, Bae GN. Langmuir. 2011; 27:10256–10264. [PubMed: 21751779]
175. Zodrow K, Brunet L, Mahendra S, Li D, Zhang A, Li Q, Alvarez PJJ. Water Research. 2009; 43:715–723. [PubMed: 19046755]
176. Zhang F, Wu XL, Chen YY, Lin H. Fibers and Polymers. 2009; 10:496–501.
177. Homan KA, Souza M, Truby R, Luke GP, Green C, Vreeland E, Emelianov S. ACS Nano. 2012; 6:641–650. [PubMed: 22188516]
178. Riaz Ahmed KB, Nagy AM, Brown RP, Zhang Q, Malghan SG, Goering PL. Toxicology in Vitro. 2017; 38:179–192. [PubMed: 27816503]
179. Prabhu S, Poulose EK. International Nano Letters. 2012; 2:32.
180. Li Y, Qin T, Ingle T, Yan J, He W, Yin JJ, Chen T. Arch Toxicol. 2017; 91:509–519. [PubMed: 27180073]
181. Arora S, Jain J, Rajwade JM, Paknikar KM. Toxicology and Applied Pharmacology. 2009; 236:310–318. [PubMed: 19269301]
182. Piao MJ, Kang KA, Lee IK, Kim HS, Kim S, Choi JY, Choi J, Hyun JW. Toxicology Letters. 2011; 201:92–100. [PubMed: 21182908]
183. Foldbjerg R, Dang DA, Autrup H. Arch Toxicol. 2011; 85:743–750. [PubMed: 20428844]
184. Chairuangkitti P, Lawanprasert S, Roytrakul S, Aueviriyavit S, Phummiratch D, Kulthong K, Chanvorachote P, Maniratanachote R. Toxicology in Vitro. 2013; 27:330–338. [PubMed: 22940466]
185. Park MV, Neigh AM, Vermeulen JP, de la Fonteyne LJ, Verharen HW, Briede JJ, van Loveren H, de Jong WH. Biomaterials. 2011; 32:9810–9817. [PubMed: 21944826]
186. Guo D, Zhu L, Huang Z, Zhou H, Ge Y, Ma W, Wu J, Zhang X, Zhou X, Zhang Y, Zhao Y, Gu N. Biomaterials. 2013; 34:7884–7894. [PubMed: 23876760]
187. Sanpui P, Chattopadhyay A, Ghosh SS. ACS Appl Mater Interfaces. 2011; 3:218–228. [PubMed: 21280584]
188. Al Gurabi MA, Ali D, Alkahtani S, Alarifi S. OncoTargets and Therapy. 2015; :295.doi: 10.2147/OTT.S77572 [PubMed: 25674004]

189. Shrivastava R, Kushwaha P, Bhutia YC, Flora S. Toxicology and Industrial Health. 2016; 32:1391–1404. [PubMed: 25548373]
190. Takata Y, Kristal AR, Santella RM, King IB, Duggan DJ, Lampe JW, Rayman MP, Blount PL, Reid BJ, Vaughan TL, Peters U. Plos One. 2012:7.
191. Lobanov AV, Hatfield DL, Gladyshev VN. Bba-Gen Subjects. 2009; 1790:1424–1428.
192. Mangiapane E, Pessione A, Pessione E. Curr Protein Pept Sc. 2014; 15:598–607. [PubMed: 24910086]
193. Arai K, Iwaoka M. Curr Org Chem. 2015; 20:155–165.
194. Lee KH, Jeong D. Mol Med Rep. 2012; 5:299–304. [PubMed: 22051937]
195. Turan B. Curr Pharm Biotechno. 2010; 11:819–836.
196. Nauser T, Dockheer S, Kissner R, Koppenol WH. Biochemistry-Us. 2006; 45:6038–6043.
197. Rooprai HK, Kyriazis I, Nuttall RK, Edwards DR, Zicha D, Aubyn D, Davies D, Gullan R, Pilkington GJ. Int J Oncol. 2007; 30:1263–1271. [PubMed: 17390030]
198. Ahmad MS, Yasser MM, Sholkamy EN, Ali AM, Mehanni MM. International Journal of Nanomedicine. 2015; 10:3389–3401. [PubMed: 26005349]
199. Weekley CM, Harris HH. Chemical Society Reviews. 2013; 42:8870–8894. [PubMed: 24030774]
200. Bath SC, Button S, Rayman MP. Brit J Nutr. 2012; 107:935–940. [PubMed: 21781365]
201. Fernandes AP, Gandin V. Bba-Gen Subjects. 2015; 1850:1642–1660.
202. Nilsonne G, Sun X, Nystrom C, Rundlof AK, Fernandes AP, Bjornstedt M, Dobra K. Free Radical Biology and Medicine. 2006; 41:874–885. [PubMed: 16934670]
203. Rayman MP. Lancet. 2012; 379:1256–1268. [PubMed: 22381456]
204. Wang HC, Riahi M, Pothen J, Bayse CA, Riggs-Gelasco P, Brumaghim JL. Inorganic Chemistry. 2011; 50:10893–10900. [PubMed: 21999616]
205. Altschmied J, Haendeler J. Antioxid Redox Sign. 2009; 11:1733–1740.
206. Bai Y, Qin BY, Zhou YH, Wang YD, Wang Z, Zheng WJ. Journal of Nanoscience and Nanotechnology. 2011; 11:5012–5017. [PubMed: 21770136]
207. Karadjova I, Dakova I, Yordanova T, Vasileva P. Journal of Analytical Atomic Spectrometry. 2016; 31:1949–1973.
208. Skalickova S, Milosavljevic V, Cihalova K, Horky P, Richtera L, Adam V. Nutrition. 2017; 33:83–90. [PubMed: 27356860]
209. Wadhwani SA, Shedbalkar UU, Singh R, Chopade BA. Appl Microbiol Biot. 2016; 100:2555–2566.
210. Zheng CP, Wang JS, Liu YN, Yu QQ, Liu Y, Deng N, Liu J. Advanced Functional Materials. 2014; 24:6872–6883.
211. Zhang J, Wang H, Bao Y, Zhang L. Life Sci. 2004; 75:237–244. [PubMed: 15120575]
212. Hassan CE, Webster TJ. International Journal of Nanomedicine. 2016; 11:3641–3654. [PubMed: 27536104]
213. Wang Q, Webster TJ. Advanced Processing and Manufacturing Technologies for Nanostructured and Multifunctional Materials. 2015:213–218.
214. Chaudhary S, Umar A, Mehta SK. Prog Mater Sci. 2016; 83:270–329.
215. Srivastava N, Mukhopadhyay M. Powder Technol. 2013; 244:26–29.
216. Srivastava P, Kowshik M. Enzyme Microb Tech. 2016; 95:192–200.
217. Luo H, Wang F, Bai Y, Chen T, Zheng W. Colloids Surf B Biointerfaces. 2012; 94:304–308. [PubMed: 22377217]
218. Tan L, Jia X, Jiang X, Zhang Y, Tang H, Yao S, Xie Q. Biosens Bioelectron. 2009; 24:2268–2272. [PubMed: 19101136]
219. Chen T, Wong YS, Zheng W, Bai Y, Huang L. Colloid Surface B. 2008; 67:26–31.
220. Hassanin KM, Abd El-Kawi SH, Hashem KS. Int J Nanomedicine. 2013; 8:1713–1720. [PubMed: 23658489]
221. Wu H, Zhu H, Li X, Liu Z, Zheng W, Chen T, Yu B, Wong KH. J Agric Food Chem. 2013; 61:9859–9866. [PubMed: 24053442]

222. Liao WZ, Yu ZQ, Lin ZH, Lei ZG, Ning ZX, Regenstein JM, Yang JG, Ren JY. Scientific Reports. 2015:5.
223. Zheng JS, Zheng SY, Zhang YB, Yu B, Zheng W, Yang F, Chen T. Colloids Surf B Biointerfaces. 2011; 83:183–187. [PubMed: 21145219]
224. Yu B, Zhang Y, Zheng W, Fan C, Chen T. Inorg Chem. 2012; 51:8956–8963. [PubMed: 22873404]
225. Pi J, Jin H, Liu R, Song B, Wu Q, Liu L, Jiang J, Yang F, Cai H, Cai J. Appl Microbiol Biotechnol. 2013; 97:1051–1062. [PubMed: 22945264]
226. Huang Y, He L, Liu W, Fan C, Zheng W, Wong YS, Chen T. Biomaterials. 2013; 34:7106–7116. [PubMed: 23800743]
227. Li YH, Li XL, Wong YS, Chen TF, Zhang HB, Liu CR, Zheng WJ. Biomaterials. 2011; 32:9068–9076. [PubMed: 21864903]
228. Moghaddam LK, Paschepari SR, Zaimy MA, Abdalaian A, Jebali A. Cancer Gene Ther. 2016; 23:321–325. [PubMed: 27608774]
229. Mary TA, Shanthi K, Vimala K, Soundarapandian K. Rsc Advances. 2016; 6:22936–22949.
230. Liu XJ, Deng GY, Wang YY, Wang Q, Gao ZF, Sun YG, Zhang WL, Lu J, Hu JQ. Nanoscale. 2016; 8:8536–8541. [PubMed: 27072410]
231. Zhang W, Lin WH, Pei Q, Hu XL, Xie ZG, Jing XB. Chemistry of Materials. 2016; 28:4440–4446.
232. Huang XQ, Chen X, Chen QC, Yu QQ, Sun DD, Liu J. Acta Biomaterialia. 2016; 30:397–407. [PubMed: 26518106]
233. Chaudhary S, Umar A, Mehta SK. Journal of Biomedical Nanotechnology. 2014; 10:3004–3042. [PubMed: 25992427]
234. Wang YH, Hao H, Li Y, Zhang SM. Colloid Surface B. 2016; 140:297–306.
235. Sengupta J, Ghosh S, Datta P, Gomes A, Gomes A. Journal of Nanoscience and Nanotechnology. 2014; 14:990–1006. [PubMed: 24730316]
236. Kumar GS, Kulkarni A, Khurana A, Kaur J, Tikoo K. Chemico-Biological Interactions. 2014; 223:125–133. [PubMed: 25301743]
237. Zhang JN, Zhou XB, Yu QQ, Yang LC, Sun DD, Zhou YH, Liu J. Acs Applied Materials & Interfaces. 2014; 6:8475–8487. [PubMed: 24758520]
238. Yang LC, Chen QC, Liu Y, Zhang JN, Sun DD, Zhou YH, Liu J. Journal of Materials Chemistry B. 2014; 2:1977–1987.
239. Novoselov KS, Geim AK, Morozov SV, Jiang D, Zhang Y, Dubonos SV, Grigorieva IV, Firsov AA. Science. 2004; 306:666–669. [PubMed: 15499015]
240. Lee C, Wei XD, Kysar JW, Hone J. Science. 2008; 321:385–388. [PubMed: 18635798]
241. Bolotin KI, Sikes KJ, Jiang Z, Klima M, Fudenberg G, Hone J, Kim P, Stormer HL. Solid State Commun. 2008; 146:351–355.
242. Du X, Skachko I, Barker A, Andrei EY. Nature Nanotechnology. 2008; 3:491–495.
243. Pop E, Varshney V, Roy AK. Mrs Bulletin. 2012; 37:1273–1281.
244. Sanchez VC, Jachak A, Hurt RH, Kane AB. Chem Res Toxicol. 2012; 25:15–34. [PubMed: 21954945]
245. Hong GS, Diao SO, Antaris AL, Dai HJ. Chemical Reviews. 2015; 115:10816–10906. [PubMed: 25997028]
246. Zhang YB, Petibone D, Xu Y, Mahmood M, Karmakar A, Casciano D, Ali S, Biris AS. Drug Metab Rev. 2014; 46:232–246. [PubMed: 24506522]
247. Bhattacharya K, Mukherjee SP, Gallud A, Burkert SC, Bistarelli S, Bellucci S, Bottini M, Star A, Fadeel B. Nanomed-Nanotechnol. 2016; 12:333–351.
248. Caffo M, Merlo L, Marino D, Caruso G. Nanomedicine. 2015; 10:1848–1848. [PubMed: 26080703]
249. Feng LZ, Liu ZA. Nanomedicine. 2011; 6:317–324. [PubMed: 21385134]
250. Mao HY, Laurent S, Chen W, Akhavan O, Imani M, Ashkarran AA, Mahmoudi M. Chemical Reviews. 2013; 113:3407–3424. [PubMed: 23452512]

251. Pattnaik S, Swain K, Lin ZQ. Journal of Materials Chemistry B. 2016; 4:7813–7831.
252. Rahman M, Akhter S, Ahmad MZ, Ahmad J, Addo RT, Ahmad FJ, Pichon C. Nanomedicine. 2015; 10:2405–2422. [PubMed: 26252175]
253. Shen H, Zhang LM, Liu M, Zhang ZJ. Theranostics. 2012; 2:283–294. [PubMed: 22448195]
254. Tonelli FMP, Goulart VAM, Gomes KN, Ladeira MS, Santos AK, Lorencon E, Ladeira LO, Resende RR. Nanomedicine. 2015; 10:2423–2450. [PubMed: 26244905]
255. Yang K, Feng LZ, Shi XZ, Liu Z. Chemical Society Reviews. 2013; 42:530–547. [PubMed: 23059655]
256. Zhang HC, Gruner G, Zhao YL. Journal of Materials Chemistry B. 2013; 1:2542–2567.
257. Song YJ, Qu KG, Zhao C, Ren JS, Qu XG. Advanced Materials. 2010; 22:2206–2210. [PubMed: 20564257]
258. Li RB, Mansukhani ND, Guiney LM, Ji ZX, Zhao YC, Chang CH, French CT, Miller JF, Hersam MC, Nel AE, Xia T. Acs Nano. 2016; 10:10966–10980. [PubMed: 28024366]
259. Orecchioni M, Cabizza R, Bianco A, Delogu LG. Theranostics. 2015; 5:710–723. [PubMed: 25897336]
260. Veitch NC. Phytochemistry. 2004; 65:249–259. [PubMed: 14751298]
261. Wang ZB, Lv XC, Weng J. Carbon. 2013; 62:51–60.
262. Garg B, Bisht T, Ling YC. Molecules. 2015; 20:14155–14190. [PubMed: 26248071]
263. Cherkasov A, Hilpert K, Jenssen H, Fjell CD, Waldbrook M, Mullaly SC, Volkmer R, Hancock REW. ACS Chemical Biology. 2008; 4:65–74.
264. Zou XF, Zhang L, Wang ZJ, Luo Y. Journal of the American Chemical Society. 2016; 138:2064–2077. [PubMed: 26824139]
265. Akhavan O, Ghaderi E. ACS Nano. 2010; 4:5731–5736. [PubMed: 20925398]
266. Liu S, Hu M, Zeng TH, Wu R, Jiang R, Wei J, Wang L, Kong J, Chen Y. Langmuir. 2012; 28:12364–12372. [PubMed: 22827339]
267. Liu S, Zeng TH, Hofmann M, Burcombe E, Wei J, Jiang R, Kong J, Chen Y. ACS Nano. 2011; 5:6971–6980. [PubMed: 21851105]
268. Tu YS, Lv M, Xiu P, Huynh T, Zhang M, Castelli M, Liu ZR, Huang Q, Fan CH, Fang HP, Zhou RH. Nature Nanotechnology. 2013; 8:594–601.
269. Li YF, Yuan HY, von dem Bussche A, Creighton M, Hurt RH, Kane AB, Gao HJ. Proceedings of the National Academy of Sciences of the United States of America. 2013; 110:12295–12300. [PubMed: 23840061]
270. Carpio IEM, Santos CM, Wei X, Rodrigues DF. Nanoscale. 2012; 4:4746–4756. [PubMed: 22751735]
271. Ruiz ON, Fernando KA, Wang B, Brown NA, Luo PG, McNamara ND, Vangsness M, Sun YP, Bunker CE. ACS Nano. 2011; 5:8100–8107. [PubMed: 21932790]
272. Palmieri V, Carmela Lauriola M, Ciasca G, Conti C, De Spirito M, Papi M. Nanotechnology. 2017; 28:152001. [PubMed: 28303804]
273. Kim TI, Kwon B, Yoon J, Park IJ, Bang GS, Park Y, Seo YS, Choi SY. ACS Appl Mater Interfaces. 2017; 9:7908–7917. [PubMed: 28198615]
274. Liu XY, Sen S, Liu JY, Kulaots I, Geohegan D, Kane A, Puretzky AA, Rouleau CM, More KL, Palmore GTR, Hurt RH. Small. 2011; 7:2775–2785. [PubMed: 21818846]
275. Perreault F, de Faria AF, Nejati S, Elimelech M. Acs Nano. 2015; 9:7226–7236. [PubMed: 26091689]
276. Gurunathan S, Han JW, Dayem AA, Eppakayala V, Kim JH. International Journal of Nanomedicine. 2012; 7:5901–5914. [PubMed: 23226696]
277. Nanda SS, An SSA, Yi DK. International Journal of Nanomedicine. 2015; 10:549–556. [PubMed: 25609960]
278. Sun HJ, Gao N, Dong K, Ren JS, Qu XG. Acs Nano. 2014; 8:6202–6210. [PubMed: 24870970]
279. Li Y, Dong HQ, Li YY, Shi DL. International Journal of Nanomedicine. 2015; 10:2451–2459. [PubMed: 25848263]

280. Yin R, Agrawal T, Khan U, Gupta GK, Rai V, Huang YY, Hamblin MR. Nanomedicine. 2015; 10:2379–2404. [PubMed: 26305189]
281. Ge JC, Lan MH, Zhou BJ, Liu WM, Guo L, Wang H, Jia QY, Niu GL, Huang X, Zhou HY, Meng XM, Wang PF, Lee CS, Zhang WJ, Han XD. Nature Communications. 2014:5.
282. Ristic BZ, Milenkovic MM, Dakic IR, Todorovic-Markovic BM, Milosavljevic MS, Budimir MD, Paunovic VG, Dramicanin MD, Markovic ZM, Trajkovic VS. Biomaterials. 2014; 35:4428–4435. [PubMed: 24612819]
283. Zhou L, Ge XF, Zhou JH, Wei SH, Shen J. Chemical Communications. 2015; 51:421–424. [PubMed: 25407475]
284. Choi HS, Liu W, Misra P, Tanaka E, Zimmer JP, Itty Ipe B, Bawendi MG, Frangioni JV. Nat Biotechnol. 2007; 25:1165–1170. [PubMed: 17891134]
285. Kotchey GP, Hasan SA, Kapralov AA, Ha SH, Kim K, Shvedova AA, Kagan VE, Star A. Accounts of Chemical Research. 2012; 45:1770–1781. [PubMed: 22824066]
286. Kotchey GP, Allen BL, Vedala H, Yanamala N, Kapralov AA, Tyurina YY, Klein-Seetharaman J, Kagan VE, Star A. Acs Nano. 2011; 5:2098–2108. [PubMed: 21344859]
287. Pantarotto D, Briand JP, Prato M, Bianco A. Chem Commun (Camb). 2004; :16–17.doi: 10.1039/b311254c [PubMed: 14737310]
288. Shi Kam NW, Jessop TC, Wender PA, Dai H. Journal of the American Chemical Society. 2004; 126:6850–6851. [PubMed: 15174838]
289. Meng J, Song L, Meng J, Kong H, Zhu G, Wang C, Xu L, Xie S, Xu H. Journal of Biomedical Materials Research Part A. 2006; 79A:298–306.
290. Correa-Duarte MA, Wagner N, Rojas-Chapana J, Morsczeck C, Thie M, Giersig M. Nano Letters. 2004; 4:2233–2236.
291. Scrivens WA, Tour JM, Creek KE, Pirisi L. Journal of the American Chemical Society. 1994; 116:4517–4518.
292. Barone PW, Baik S, Heller DA, Strano MS. Nat Mater. 2005; 4:86–92. [PubMed: 15592477]
293. Cherukuri P, Bachilo SM, Litovsky SH, Weisman RB. Journal of the American Chemical Society. 2004; 126:15638–15639. [PubMed: 15571374]
294. Heller DA, Baik S, Eurell TE, Strano MS. Advanced Materials. 2005; 17:2793–2799.
295. Mauter MS, Elimelech M. Environmental Science & Technology. 2008; 42:5843–5859. [PubMed: 18767635]
296. Kroto HW, Heath JR, O'Brien SC, Curl RF, Smalley RE. Nature. 1985; 318:162–163.
297. Haddon RC, Perel AS, Morris RC, Palstra TTM, Hebard AF, Fleming RM. Applied Physics Letters. 1995; 67:121–123.
298. David T, Gimzewski JK, Purdie D, Reihl B, Schlittler RR. Physical Review B. 1994; 50:5810–5813.
299. Hunt MRC, Modesti S, Rudolf P, Palmer RE. Physical Review B. 1995; 51:10039–10047.
300. Bethune DS, Johnson RD, Salem JR, de Vries MS, Yannoni CS. Nature. 1993; 366:123–128.
301. Saito R, Fujita M, Dresselhaus G, Dresselhaus MS. Applied Physics Letters. 1992; 60:2204–2206.
302. Ebbesen TW, Tanigaki K, Kuroshima S. Chemical Physics Letters. 1991; 181:501–504.
303. Dresselhaus, MS., Dresselhaus, G., Eklund, PC. Science of Fullerenes and Carbon Nanotubes. Academic Press; San Diego: 1996. p. 15-59.DOI: http://dx.doi.org/10.1016/B978-012221820-0/50002-2
304. Goel A, Howard JB, Vander Sande JB. Carbon. 2004; 42:1907–1915.
305. Xu X, Ray R, Gu Y, Ploehn HJ, Gearheart L, Raker K, Scrivens WA. J Am Chem Soc. 2004; 126:12736–12737. [PubMed: 15469243]
306. Dresselhaus, MS., Dresselhaus, G., Eklund, PC. Science of Fullerenes and Carbon Nanotubes. Academic Press; San Diego: 1996. p. 171-223.DOI: http://dx.doi.org/10.1016/B978-012221820-0/50007-1
307. Dresselhaus MS, Dresselhaus G, Saito R. Carbon. 1995; 33:883–891.
308. Wang Y, Hu A. Journal of Materials Chemistry C. 2014; 2:6921–6939.

309. Iijima S, Yudasaka M, Yamada R, Bandow S, Suenaga K, Kokai F, Takahashi K. Chemical Physics Letters. 1999; 309:165–170.

310. Kagan VE, Konduru NV, Feng W, Allen BL, Conroy J, Volkov Y, Vlasova II, Belikova NA, Yanamala N, Kapralov A, Tyurina YY, Shi J, Kisin ER, Murray AR, Franks J, Stolz D, Gou P, Klein-Seetharaman J, Fadeel B, Star A, Shvedova AA. Nat Nano. 2010; 5:354–359.

311. Allen BL, Kichambare PD, Gou P, Vlasova, Kapralov AA, Konduru N, Kagan VE, Star A. Nano Lett. 2008; 8:3899–3903. [PubMed: 18954125]

312. Li Z, Wang Y, Kozbial A, Shenoy G, Zhou F, McGinley R, Ireland P, Morganstein B, Kunkel A, Surwade SP, Li L, Liu H. Nat Mater. 2013; 12:925–931. [PubMed: 23872731]

313. Rafiee J, Mi X, Gullapalli H, Thomas AV, Yavari F, Shi Y, Ajayan PM, Koratkar NA. Nat Mater. 2012; 11:217–222. [PubMed: 22266468]

314. Xu K, Heath JR. Nat Mater. 2013; 12:872–873. [PubMed: 24056851]

315. Unwin PR, Güell AG, Zhang G. Accounts of Chemical Research. 2016; 49:2041–2048. [PubMed: 27501067]

316. Tasis D, Tagmatarchis N, Bianco A, Prato M. Chemical Reviews. 2006; 106:1105–1136. [PubMed: 16522018]

317. Pleskov YV, Evstefeeva YE, Krotova MD, Elkin VV, Baranov AM, Dement'ev AP. Diamond and Related Materials. 1999; 8:64–72.

318. Hance GW, Kuwana T. Analytical Chemistry. 1987; 59:131–134.

319. Hartleb H, Späth F, Hertel T. ACS Nano. 2015; doi: 10.1021/acsnano.5b04707

320. Kavan L, Rapta P, Dunsch L, Bronikowski MJ, Willis P, Smalley RE. The Journal of Physical Chemistry B. 2001; 105:10764–10771.

321. Schafer S, Cogan NM, Krauss TD. Nano Lett. 2014; 14:3138–3144. [PubMed: 24797608]

322. Tanaka Y, Hirana Y, Niidome Y, Kato K, Saito S, Nakashima N. Angew Chem Int Ed Engl. 2009; 48:7655–7659. [PubMed: 19739154]

323. Kavan L, Dunsch L. ChemPhysChem. 2011; 12:47–55. [PubMed: 21226179]

324. Echegoyen L, Echegoyen LE. Accounts of Chemical Research. 1998; 31:593–601.

325. Aguirre CM, Levesque PL, Paillet M, Lapointe F, St-Antoine BC, Desjardins P, Martel R. Advanced Materials. 2009; 21:3087–3091.

326. Wang S, Yu D, Dai L. Journal of the American Chemical Society. 2011; 133:5182–5185. [PubMed: 21413707]

327. Pascal-Levy Y, Shifman E, Pal-Chowdhury M, Kalifa I, Rabkin T, Shtempluck O, Razin A, Kochetkov V, Yaish YE. Physical Review B. 2012; 86:115444.

328. Giannozzi P, Car R, Scoles G. The Journal of Chemical Physics. 2003; 118:1003–1006.

329. Collins PG, Bradley K, Ishigami M, Zettl A. Science. 2000; 287:1801–1804. [PubMed: 10710305]

330. Lu Z, Dai T, Huang L, Kurup DB, Tegos GP, Jahnke A, Wharton T, Hamblin MR. Nanomedicine (Lond). 2010; 5:1525–1533. [PubMed: 21143031]

331. Tegos GP, Demidova TN, Arcila-Lopez D, Lee H, Wharton T, Gali H, Hamblin MR. Chemistry & biology. 2005; 12:1127–1135. [PubMed: 16242655]

332. Song, C., Zhang, J. PEM Fuel Cell Electrocatalysts and Catalyst Layers: Fundamentals and Applications. Zhang, J., editor. Springer London; London: 2008. p. 89-134.

333. Kim SE, Zhang L, Ma K, Riegman M, Chen F, Ingold I, Conrad M, Turker MZ, Gao M, Jiang X, Monette S, Pauliah M, Gonen M, Zanzonico P, Quinn T, Wiesner U, Bradbury MS, Overholtzer M. Nat Nano. 2016; 11:977–985.

334. Huq R, Samuel ELG, Sikkema WKA, Nilewski LG, Lee T, Tanner MR, Khan FS, Porter PC, Tajhya RB, Patel RS, Inoue T, Pautler RG, Corry DB, Tour JM, Beeton C. Scientific Reports. 2016; 6:33808. [PubMed: 27654170]

335. Berlin JM, Leonard AD, Pham TT, Sano D, Marcano DC, Yan S, Fiorentino S, Milas ZL, Kosynkin DV, Price BK, Lucente-Schultz RM, Wen X, Raso MG, Craig SL, Tran HT, Myers JN, Tour JM. ACS Nano. 2010; 4:4621–4636. [PubMed: 20681596]

336. Bitner BR, Marcano DC, Berlin JM, Fabian RH, Cherian L, Culver JC, Dickinson ME, Robertson CS, Pautler RG, Kent TA, Tour JM. ACS nano. 2012; 6:8007–8014. [PubMed: 22866916]
337. Cheng Y, Jiang SP. Progress in Natural Science: Materials International. 2015; 25:545–553.
338. Wang J, Nguyen TD, Cao Q, Wang Y, Tan MYC, Chan-Park MB. ACS Nano. 2016; 10:3222–3232. [PubMed: 26901408]
339. Kim SM, Kim KK, Jo YW, Park MH, Chae SJ, Duong DL, Yang CW, Kong J, Lee YH. ACS Nano. 2011; 5:1236–1242. [PubMed: 21207986]
340. Sabri SS, Lévesque PL, Aguirre CM, Guillemette J, Martel R, Szkopek T. Applied Physics Letters. 2009; 95:242104.
341. Barboza APM, Gomes AP, Archanjo BS, Araujo PT, Jorio A, Ferlauto AS, Mazzoni MSC, Chacham H, Neves BRA. Physical Review Letters. 2008; 100:256804. [PubMed: 18643691]
342. Hou W-C, BeigzadehMilani S, Jafvert CT, Zepp RG. Environmental Science & Technology. 2014; 48:3875–3882. [PubMed: 24628431]
343. Hsieh H-S, Jafvert CT. Carbon. 2015; 89:361–371.
344. Jespersen TS, Nygard J. Nano Lett. 2005; 5:1838–1841. [PubMed: 16159234]
345. Hsieh H-S, Wu R, Jafvert CT. Environmental Science & Technology. 2014; 48:11330–11336. [PubMed: 25171301]
346. Chen C-Y, Jafvert CT. Environmental Science & Technology. 2010; 44:6674–6679. [PubMed: 20687543]
347. Petersen EJ, Tu X, Dizdaroglu M, Zheng M, Nelson BC. Small. 2013; 9:205–208. [PubMed: 22987483]
348. Zheng M, Diner BA. Journal of the American Chemical Society. 2004; 126:15490–15494. [PubMed: 15563177]
349. Guldi DM, Taieb H, Rahman GMA, Tagmatarchis N, Prato M. Advanced Materials. 2005; 17:871–875.
350. Marty L, Adam E, Albert L, Doyon R, Ménard D, Martel R. Physical Review Letters. 2006; 96:136803. [PubMed: 16712017]
351. Yuma B, Berciaud S, Besbas J, Shaver J, Santos S, Ghosh S, Weisman RB, Cognet L, Gallart M, Ziegler M, Hönerlage B, Lounis B, Gilliot P. Physical Review B. 2013; 87:205412.
352. Soavi G, Scotognella F, Viola D, Hefner T, Hertel T, Cerullo G, Lanzani G. Scientific Reports. 2015; 5:9681. [PubMed: 25959462]
353. Park J, Reid OG, Blackburn JL, Rumbles G. Nat Commun. 2015:6.
354. Olivier J-H, Park J, Deria P, Rawson J, Bai Y, Kumbhar AS, Therien MJ. Angewandte Chemie International Edition. 2015; 54:8133–8138. [PubMed: 26014277]
355. Silvera-Batista CA, Wang RK, Weinberg P, Ziegler KJ. Physical Chemistry Chemical Physics. 2010; 12:6990–6998. [PubMed: 20463994]
356. OCMJ, Eibergen EE, Doorn SK. Nat Mater. 2005; 4:412–418. [PubMed: 15821741]
357. Crochet JJ, Duque JG, Werner JH, Doorn SK. Nat Nanotechnol. 2012; 7:126–132. [PubMed: 22231665]
358. Satishkumar BC, Brown LO, Gao Y, Wang C-C, Wang H-L, Doorn SK. Nat Nano. 2007; 2:560–564.
359. Joshi A, Punyani S, Bale SS, Yang H, Borca-Tasciuc T, Kane RS. Nat Nano. 2008; 3:41–45.
360. González-Durruthy M, Castro M, Nunes SM, Ventura-Lima J, Alberici LC, Naal Z, Atique-Sawazaki DT, Curti C, Ruas CP, Gelesky MA, Roy K, González-Díaz H, Monserrat JM. Carbon. 2017; 115:312–330.
361. Giraldo JP, Landry MP, Faltermeier SM, McNicholas TP, Iverson NM, Boghossian AA, Reuel NF, Hilmer AJ, Sen F, Brew JA, Strano MS. Nat Mater. 2014; 13:400–408. [PubMed: 24633343]
362. Chen C, Li Y-F, Qu Y, Chai Z, Zhao Y. Chemical Society Reviews. 2013; 42:8266–8303. [PubMed: 23868609]
363. Lim SY, Shen W, Gao Z. Chemical Society Reviews. 2015; 44:362–381. [PubMed: 25316556]
364. Miyawaki J, Yudasaka M, Azami T, Kubo Y, Iijima S. ACS Nano. 2008; 2:213–226. [PubMed: 19206621]

365. Horie M, Komaba LK, Fukui H, Kato H, Endoh S, Nakamura A, Miyauchi A, Maru J, Miyako E, Fujita K, Hagihara Y, Yoshida Y, Iwahashi H. Carbon. 2013; 54:155–167.

366. Sandanayaka ASD, Ito O, Zhang M, Ajima K, Iijima S, Yudasaka M, Murakami T, Tsuchida K. Advanced Materials. 2009; 21:4366–4371. [PubMed: 26042946]

367. Drezek RA, Tour JM. Nat Nano. 2010; 5:168–169.

368. Zheng M. Topics in Current Chemistry. 2017; 375:13. [PubMed: 28083771]

369. Worle-Knirsch JM, Pulskamp K, Krug HF. Nano Lett. 2006; 6:1261–1268. [PubMed: 16771591]

370. Love SA, Maurer-Jones MA, Thompson JW, Lin YS, Haynes CL. Annu Rev Anal Chem. 2012; 5:181–205.

371. Sharifi S, Behzadi S, Laurent S, Forrest ML, Stroeve P, Mahmoudi M. Chemical Society Reviews. 2012; 41:2323–2343. [PubMed: 22170510]

372. Yildirimer L, Thanh NTK, Loizidou M, Seifalian AM. Nano Today. 2011; 6:585–607. [PubMed: 23293661]

373. Fadeel B. Journal of Internal Medicine. 2013; 274:578–580. [PubMed: 24102766]

374. Nel A, Xia T, Meng H, Wang X, Lin SJ, Ji ZX, Zhang HY. Accounts of Chemical Research. 2013; 46:607–621. [PubMed: 22676423]

375. Nel AE. Journal of Internal Medicine. 2013; 274:561–577. [PubMed: 23879741]

376. Nel AE, Nasser E, Godwin H, Avery D, Bahadori T, Bergeson L, Beryt E, Bonner JC, Boverhof D, Carter J, Castranova V, DeShazo JR, Hussain SM, Kane AB, Klaessig F, Kuempel E, Lafranconi M, Landsiedel R, Malloy T, Miller MB, Morris J, Moss K, Oberdorster G, Pinkerton K, Pleus RC, Shatkin JA, Thomas R, Tolaymat T, Wang A, Wong J. Acs Nano. 2013; 7:6422–6433. [PubMed: 23924032]

377. Nelson BC, Wright CW, Ibuki Y, Moreno-Villanueva M, Karlsson HL, Hendriks G, Sims CM, Singh N, Doak SH. Mutagenesis. 2017; 32:215–232. [PubMed: 27565834]

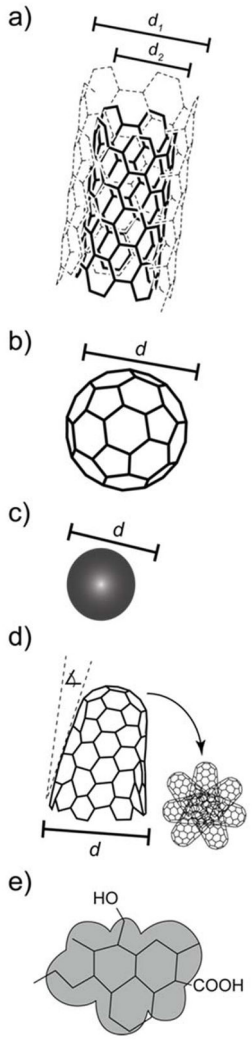

Figure 1.

(a) A carbon nanotube. The d_2 diameter indicates a single-walled material, whereas d_1 indicates the total diameter of a double-walled material. Multi-walled CNTs consist of additional lattice layers, (b) A carbon Bucky Fullerene with diameter *d.* (c) A carbon quantum dot with diameter *d.* (d) A single-walled carbon nanohorn segment of diameter d which tapers at an angle towards its tip. The arrow points towards the aggregate star structure. (e) An amorphous carbon particle with hydrophilic oxygen functionalities (hydroxyl: OH, carboxylic: COOH).